Oznaka poročila: ARRS-RPROJ-ZP-2011-1/57

ZAKLJUČNO POROČILO O REZULTATIH RAZISKOVALNEGA PROJEKTA

A. PODATKI O RAZISKOVALNEM PROJEKTU

1. Osnovni podatki o raziskovalnem projektu

Šifra projekta	J7-0363	
Naslov projekta	Naravni in antropogeni sevalci gama in beta v podzemnih vodah Slovenije	
Vodja projekta	2586	Matjaž Aleš Korun
Tip projekta	J	Temeljni projekt
Obseg raziskovalnih ur	4.170	
Cenovni razred	D	
Trajanje projekta	02.2008 - 01.2011	
Nosilna raziskovalna organizacija	106	Institut "Jožef Stefan"
Raziskovalne organizacije - soizvajalke	215 6484	Geološki zavod Slovenije JAVNO PODJETJE VODOVOD-KANALIZACIJA, d.o.o.
Družbeno-ekonomski cilj	13.	Splošni napredek znanja - RiR financiran iz drugih virov (ne iz splošnih univerzitetnih fondov - SUF)

1.1. Družbeno-ekonomski cilj[1]

Šifra	01.
Naziv	Raziskovanje in izkoriščanje zemlje

2. Sofinancerji[2]

1.	Naziv	
	Naslov	
2.	Naziv	
	Naslov	
3.	Naziv	
	Naslov	

B. REZULTATI IN DOSEŽKI RAZISKOVALNEGA PROJEKTA

3. Poročilo o realizaciji programa raziskovalnega projekta[3]

Vzorčevanje

V spomladanskem in jesenskem obdobju v letu 2010 je bilo izvedeno vzorčenje podzemne vode na različnih merilnih mestih v Sloveniji. Mreža vzorčnih mest je bila sestavljena iz izvirov, piezometrov, črpališč pitne vode, privatnih vodnjakov in deževnice. Spomladi je vzorčenje potekalo 43 vzorčnih mestih za analizo gama sevalcev ter na 45 vzorčnih mestih za analizo tritija v podzemni vodi, v jesenskem obdobju pa na 28 vzorčnih mestih za analizo gama sevalcev in analizo tritija v podzemni vodi.

Število vzorcev, zbranih tekom izvajanje projekta je v sledeči tabeli.

Leto		Število vzorcev Spektrometrija gama	Število vzorcev Scintilacijska spektrometrija
2008		10	13
2009	1. polletje	48	57
	2. polletje	39	46
2010	1. polletje	43	44
	2. polletje	28	28

Vzorci so bili odvzeti zbrani na 81 različnih lokacijah za spektrometrijo gama in na 91 lokacijah za meritve tritija.

Vzorčenje je na piezometrih, črpališčih ter privatnih vodnjakih potekalo z uporabo potopne črpalke s pretokom 0,2 l/s. Pred vzorčenjem se je iz vsakega objekta izčrpalo vsaj 1-kratni volumen stoječega vodnega stolpca ter se s tem omogočil dotok sveže vode. Med prečrpavanjem podzemne vode smo izvedli večkratne meritve fizikalno-kemijskih parametrov: električna prevodnost, pH ter temperatura vode. Ko so se merjeni parametri stabilizirali smo odvzeli vzorce vode. Vzorce izvirov smo zajeli čim bližje iztoku podzemne vode na površje. Za analizo gama sevalcev smo napolnili 50 l sod ter dodali nakisali s HNO3 na pH 2 ali manj. Za analizo tritija smo napolnili 2 plastenki po 1 l. Poleg analiz gama sevalcev in tritija so bili odvzeti tudi vzorci za osnovne fizikalno-kemijske parametre v podzemni vodi: stabilni izotopi (δ^{15}N, δ^{13}C, δ^{18}O, δ^{2}D), osnovna kemija (Fe, Ca, Mg, Na, K, NH4, HCO3, kloridi, nitrati, sulfati, fosfati) in mikroelementi (Ag, Al, As, Au, B, Ba, Be, Bi, Br, Ca, Cd, Ce, Cl, Co, Cr, Cs, Cu, Dy, Er, Eu, Fe, Ga, Gd, Ge, Hf, Hg, Ho, In, Ir, K, La, Li, Lu, Mg, Mn, Mo, Na, Nb, Nd, Ni, Os, P, Pb, Pd, Pr, Pt, Rb, Re, Rh, Ru, S, Sb, Sc, Se, Si, Sm, Sn, Sr, Ta, Tb, Te, Th, Ti, Tl, Tm, U, V, W, Y, Yb, Zn, Zr).

Tekočinskoscintilacijska spektrometrija

Meritve
V okviru projekta je bilo izmerjenih in izračunanih 165 vzorcev podzemnih vod in deževnice, od tega je 62 rezultatov povprečje dveh neodvisnih analitskih metod. 12 vzorcev je bilo pomerjenih tudi v drugih laboratorijih (Univerza v Krakowu, Poljska in Institut Euđer Bošković, Zagreb, Hrvatska). Rezultati so primerljivi in bodo predstavljeni na konferenci na Krku v sredini aprila 2011, prispevek je sprejet v objavo (Barešić 2011). Vrednosti za H-3 se gibljejo med 0 in 1400 Bq / m3.

Največ vzorcev (37) je med 688 in 788 Bq/m3. Rezultati bodo podrobneje predstavljeni in obdelani v okviru doktorata Katarine Kovačič.

Izboljšava analitske metode
Metoda za določevanje tritija po elektrolitski obogatitvi (Rozanski 2003) v izračunu ne zajema nekaterih tehničnih parametrov priprave vzorcev, ki lahko vplivajo na končno vrednost, zato na njihov račun povečamo negotovost rezultata. Pri datiranju vod si poleg čim nižje meje detekcije prizadevamo tudi za čim manjšo negotovost rezultata, saj bo tako določevanje starosti vod natančnejše. Izvedli smo vrsto poskusov, s katerimi smo podrobno študirali različne dejavnike, ki lahko vplivajo na končni izračun aktivnosti. Delni rezultati so bili predstavljeni na konferenci o LSC spektrometriji v Parizu (Kožar Logar 2010), ostali bodo podrobneje obdelani v sklopu doktorske disertacije mlade raziskovalke Katarine Kovačič, katere usposabljanje še teče.

Spektrometrija gama

Meritve s spektrometrijo gama še niso zaključene, ker je treba vzorce meriti dvakrat. Na vzorcih iz leta 2010 je treba izvesti še 58 meritev. Te meritve bomo opravili v okviru dveh doktorskih disertacij. Prav tako bomo v okviru disertacij ovrednotili rezultate in jih objavili.

Meritve vodnih vzorcev iz okolja s spektrometrijo gama so težavne, ker je koncentracija sevalcev v vodi razmeroma majhna, spektrometrija gama pa ni posebno občutljiva metoda, v primerjavi z metodami ki vključujejo radiokemijsko pripravo vzorca. Da bi izboljšali občutljivost, za pripravo merjenca uporabimo večjo količino zbranega vzorca, približno 50 L. Zbrane vzorce izparimo in merimo aktivnost suhega ostanka. Koncentracija mineralnih snovi v površinskih vodah je okrog 0.05 %, zato z izparevanjem koncentriramo radioaktivno kontaminacijo vode za faktor 2000 in pridobimo okrog 30 g suhega ostanka. Vkljub temu je aktivnost merjenca tako nizka, da predstavljajo problemi meritev in tolmačenja merskih rezultatov v bližini detekcijske meje glavno težavo. Za meritve uporabljamo le en, najobčutljivejši, spektrometer, meritev enega vzorca pa traja dva dni. Vsak vzorec pomerimo dvakrat, enkrat čim prej po vzorčevanju in po nekaj mesecih, da lahko iz časovne odvisnosti ocenimo koncentracijo Th-234 in z dvakratno meritvijo povečamo zanesljivost rezultatov. Probleme tolmačenja rezultatov in rešitve smo objavili v člankih "Interpretation of measurement results near the detection limit in gamma-ray spectrometry using Bayesian statistisc", "Probability for Type I errors in gamma-ray spectrometric measurements of drinking water samples" in "Determination of ^{238}U in ground-water samples using gamma-ray spectrometry".

Zaključek

Problematiko meritev Ra-226 pri nizkih koncentracijah smo obravanvali v delu "Background daughters in gamma-ray spectrometric measurements,", predstavljenem na konferenci "Environmental Radioactivity" v Rimu in v delu "A comparative study of the radon-induced background in low-level gamma-ray spectrometry", ki je poslano v objavo.

Preliminarne merske rezultate smo objavili v prispevku "Tritium and gamma emitters in Slovenian groundwater" na konferenci LCS 2010, International Conference on Advances in Liquid Scientillation v Parizu in v prispevku "Concentration of tritium and members of the uranium and thorium decay chains in ground water in Slovenia and their implications for managing ground water resources" na konferenci International Symposium on Isotopes in Hydrology, Marine Ecosystems, and Climate Change Studies v Monaku.

Rokopisi vseh še neobjavljenih prispevkov so v priponkah. Prav tako so v priponki merski rezultati.

Povzetek

Vsi vzorci, predvideni v projektu, so bili zbrani. Meritve še niso končane zaradi nezadostnih merskih kapacitet in ker je vzorce treba meriti večkrat. Meritve se nadaljujejo v okviru dveh doktorskih disertacij.

Vse objave, napovedane v poročilu za leto 2009 so realizirane. V objavo so poslana štiri dela, eno delo je v postopku priprave na objavo.

4. Ocena stopnje realizacije zastavljenih raziskovalnih ciljev[4]

Ocenjujemo, da smo dosegli raziskovalne cilje, zastavljene v projektu. Vse objave, napovedane v poročilu za leto 2009 so realizirane. Delo bomo nadaljevali v okviru doktorskih disertacij, ki se bodo izvajale še dve leti, na vzorčrvanju, meritvah zbranih vzorcev, pred vsem pa na izpopolnjevanju metodologije za interpretiranje rezultatov v bližini detekcijske meje, interpretacijo samih merskih rezultatov in objavljanjem publikacij.

5. Utemeljitev morebitnih sprememb programa raziskovalnega projekta oziroma

sprememb, povečanja ali zmanjšanja sestave projektne skupine[5]

Spremembe niso predvidene.

6. Najpomembnejši znanstveni rezultati projektne skupine[6]

	Znanstveni rezultat		
1.	Naslov	*SLO*	Interpretacija merskih rezultatov v bližini detekcijske meje v spektrometriji gama z Bayseiansko statistiko
		ANG	Interpretation of measurement results near the detection limit in gamma-ray spectrometry using Bayesian statistics
	Opis	*SLO*	Zahteva, da prava vrednost aktivnosti ne more biti negativna uporabimo za transformiranje izmerkov , ki so lahko pozitivni ali negativni v pričakovane vrednosti. Verjetnostna porazdelitev aktivnosti je odsekana normalna porazdelitev, pričakovano vrednost variance prave vrednosti pa dobimo iz izmerka in njegove negotovosti. Pokažemo, da je standardna deviacija prave vrednosti manjša od negotovosti izmerka in da je razmerje med standardno devijacijo pričakovane vrednosti in pričakovano vrednostjo samo manj kot ena. Ker je pričakovana vrednost vedno večja od izmerka izboljšamo rezultat.
		ANG	The requirement that the true value of an anctivity cannot be negative is used for transformation of raw observed values into expected activity values. The probability distribution of the activity values is a truncated normal distribution and the expected value and the variance of the activity value are derived from the observed value and its standard deviation. It has been shown that the standard deviation of the activity value is less than the standard deviation of the observed value and that the ratio of the standard deviation of the activity value and the expected value is less than one.
	Objavljeno v		KORUN, Matjaž, MAVER, Petra. Interpretation of the measurement results near the detection limit in gamma-ray spectrometry using Bayesian statistics. Accred. Qual. Assur. 2010, 15, 515-520
	Tipologija		1.01 Izvirni znanstveni članek
	COBISS.SI-ID		23900967
2.	Naslov	*SLO*	Verjetnost za napake tipa I pri meritvah vzorcev pitne vode s spektrometrijo gama
		ANG	Probability for Type I errors in gamma-ray spectrometric measurementrs of drinking water samples
	Opis	*SLO*	V spektrih žarkov gama, ki so bili izmerjeni v odsotnosti vzorca, se pojavijo vrhovi, ki pripadajo ozadju spektrometra. Če merimo vzorce, ki vsebujejo radionuklide, ki nastopajo tudi v ozadju, in imajo aktivnosti v bližini detekcijske meje, prispeva ozadje znatno k ploščini vrhov. Verjetnosti za napačno identificirane radionuklide z mejami za odločitve so podane za radionuklide, ki se pojavijo v ozadju spektrometrov. Za nekatere radionuklide, ki ne nastopajo v ozadju prav tako podajamo verjetnosti za napačno identifikacijo.
		ANG	In gamma-ray spectra, acquired in the absence of the sample, peaks occor which belong to the spectrometer background. When samples are measured, which contain radionuclide that appear in the background also and have activities near the detection level, the background contributes substantially to the peak areas. The probabilities for false positives together with the decision thresholds are given for radionuclides appearing in the background spectra. For some radionuclides that do not appear in the background spectra, probabilities for false detection are given as well.
	Objavljeno v		KORUN, Matjaž, KOVAČIČ, Katarina, VODENIK, Branko. Probability for type I errors in gamma-ray spectrometric measurements of drinking water samples. J. Radioanal. Nucl. Chem 2010, 286, 553-556
	Tipologija		1.01 Izvirni znanstveni članek
	COBISS.SI-ID		24131111
3.	Naslov	*SLO*	Določanje 238U v vzorcih podzemnih vod s spektrometrijo gama
		ANG	Determination of 238U in ground-water samples using gamma-ray spectrometry

	Opis	SLO	Opisan je postopek za meritve nizkih koncentracij 238U v vodi. Vzorce z volumnom 50 L smo izpareli in merili suhi ostanek. Po tem postopku smo pridobili okrog 30 g suhega ostanka. Mejo za odločitev za meritve s spektrometrijo gama smo ocenili na 1.5 Bq/m3. V 26 vzorcih smo izmerili koncentracije do 20 Bq/m3. Večina merskih rezultatov leži v območju okrog 5 Bq/m3.
		ANG	A method for measuring the low-activity concentration of 238U in water is described. Samples of 50 L were evaporated and the dry residue after evaporation was measured. Typically, 30 g of material was obtained for the samples processed in this way. The decision threshold resulting from gamma-ray spectrometric measurements was assessed to 1.5 Bq/m3. A total od 26 samples of ground awter were processed and activity concentrations up to 20 Bq/m3 were measured. However, most of the results were in the range arround 5 Bq/m3.
	Objavljeno v		KORUN, Matjaž, KOVAČIČ, Katarina. Determination of the [sup](238)U in ground-water samples using gamma-ray spectrometry. Appl. Radiat. Isot. 2011, 69, 636-640
	Tipologija		1.01 Izvirni znanstveni članek
	COBISS.SI-ID		24321319
4.	Naslov	SLO	Ozadje radonovih potomcev v meritvah spektrometrije gama
		ANG	Background of radon daughters in gamma-ray spectrometric measurements
	Opis	SLO	K ozadju radonovih potomcev prispevajo razni viri, ki so na raznih delih spektrometra. Ozadje spektrometra zaradi radonovih potomcev izvira iz 226Ra v detektorju in ščitu, prisotnosti radonovih potomcev v zraku v notranjosti ščita in v nepopolni atenuaciji žarkov, ki prihajajo iz okolice spektrometra. Ugotovili smo, da je pri nekaterih detektorjih ozadje zaradi radonovih potomcev od časa neodvisno, pri nekaterih pa je korelirano z zunanjo temperaturo.
		ANG	The background due to radon daughters originates from various sources, characterized by the location of radon daughters in the spectrometer. The spectrometer background due to radon daughters originates in the presence of 226Ra in the detector and the shielding, the presence of radon daughters in the air filling the shield's cavity and in the incomplete attenuation of gamma-rays from the environment where the shield is situated. It was found that in some detectors background induced by radon daughters is constant in time whereas in others it exhibits correlation with outside temperature.
	Objavljeno v		MAVER, Petra, KORUN, Matjaž, MARTELANC, Matej, VODENIK, Branko. Background of radon daughters in gamma-ray spectrometric measurements. V: Enviroinmental radioactivity 2010, 25-27 October 2010, Rome, Italy. Book of abstracts : new frontiers and developments.
	Tipologija		1.08 Objavljeni znanstveni prispevek na konferenci
	COBISS.SI-ID		24430631
5.	Naslov	SLO	Tritij in sevalci gama v podzemnih vodah Slovenije
		ANG	Tritium and gamma emitters in Slovenian groundawter
	Opis	SLO	V podzemskih vodah Slovenije smo izmerili koncentracije tritija, sevalcev gama v uranovem in torijevem razpadnem nizu (U-238, Th-234, Pb-210, Ra-228 in Th-228) in kalija. Opazili smo korelacije med koncentracijami Ra-226, Ra-228 in Th-228 v vzorcih iz medzrnskih in razpoklinskih vodonosnikov. Opazili smo tudi, da je razpon koncentracij tritija v medzrnskih vodonosnikih največji, najmanjši pa v razpoklinskih.
		ANG	Concentrations of tritium, gamma-ray emitters in the uranium and thorium decay chains (U-238, Th-234, Pb-210, Ra-228, Ra-226 and Th-228) and potassium were measured in samples of ground water in Slovenia. Correlations among Ra-226, Ra-228 and Th-228 were observed in samples from intergranular and fractured aquifers. It was also found that the variability of tritium activity in intergranular aquifers is the largerestand in fractured ones the smallest.
	Objavljeno v		KOVAČIČ, Katarina, KOŽAR LOGAR, Jasmina, KORUN, Matjaž. Tritium and gamma emitters in Slovenian groundwater. LSC 2010, International Conference on Advences on Liquid Scintillation spectrometry, September 6-10, Paris, France. Programme and abstracts.

	Tipologija	1.08 Objavljeni znanstveni prispevek na konferenci
	COBISS.SI-ID	24327207

7. Najpomembnejši družbeno-ekonomsko relevantni rezultati projektne skupine[6]

	Družbeno-ekonomsko relevantni rezultat		
1.	Naslov	*SLO*	Vodenje projekta INCOME (LIFE07/SLO/ENV/000725)
		ANG	Management of INCOME project (LIFE07/SLO/ENV/000725)
	Opis	*SLO*	Namen projekta INCOME je vzpostavitev postopkov za učinkovito upravljanje z onesnaženimi vodonosniki. Projekt povezuje postopke za odkrivanje in nadzor virov onesnaževanja in ukrepe za izboljšanje stanja. Osnovna cilja projekta INCOME sta razvoj integriranega sistema za podporo v odločanju (DSS) in predlog izvedljivega in sprejemljivega programa aktivnosti za podporo upravljanju z občutljivo ''urbano'' podzemno vodo v aluvialnih vodonosnikih pod visoko urbaniziranim področjem Mestne občine Ljubljana.
		ANG	The INCOME project is intended for the establishment of an effective management of contaminated aquifers. The project connects procedures for discovering and supervising sources of pollution, and measures for improving the condition. The two primary objectives of the project are to develop an integrated decision making support system (DSS) and the proposal of a feasible/accepted program of activities for sustainable management of extremely vulnerable "urban" groundwater in the alluvial aquifer below the highly urbanized area of the Municipality of Ljubljana.
	Šifra		D.01 Vodenje/koordiniranje (mednarodnih in domačih) projektov
	Objavljeno v		JAMNIK, Brigita. Jasni ukrepi za dolgoročno izboljšanje stanja vodnih virov : evropski okoljevarstveni projekt INCOME. Ljubljana, oktober 2010, letn. 15, št. 7, str. 32.
	Tipologija		1.04 Strokovni članek
	COBISS.SI-ID		1866069
2.	Naslov	*SLO*	Ustanovitev in postavitev raziskovalnega Laboratorija za tekočinskoscintilacijsko spektrometrijo
		ANG	Establishment of low-level tritium laboratory
	Opis	*SLO*	Po tem, ko smo namestili opremo, smo analizirali zaporedje operacij, potrebnih za izvedbo analiznega postopka (vzorčevanje, konzerviranje vzorcev, prva destilacija, elektrolitska obogatitev, druga destilacija, priprava meritev in kontrolnih vzorcev, štetje in ocena rezultatov). Identificirali smo glavne vire negotovosti. Analitski proces smo preverili v nekaj mednarodnih primerjalnih meritvah in testih usposobljenosti. V prispevku predstavljamo rezultate in dileme, ki so se pojavile pri postavitvi laboratorija.
		ANG	After installing the equipment the sequence of steps (sampling, conservation of samples, first distillation, electrolytical enrichment, second distillation, preparation of measurements and control samples, LSC counting, calculation and evaluation of the results) necessary to carry out the analytical procedure were analyzed. The main sources of uncertainties were identified. The analytical process was checked in several international intercomparisons and proficiency tests. The results and dilemmas that came up during the establishment of the laboratory are presented.
	Šifra		D.02 Ustanovitev raziskovalnega centra, laboratorija, študija, društva
	Objavljeno v		KOŽAR LOGAR, Jasmina, GLAVIČ-CINDRO, Denis. Establishment of low-level tritium laboratory. V: EIKENBERG, Jost (ur.). LSC 2008, advances in liquid scintillation spectrometry : proceedings of the 2008 International Liquid Scintillation Conference, Davos, Switzerland, 25-30 May 2008. Tucson: Radiocarbon, 2009, str. 241-249.
	Tipologija		1.08 Objavljeni znanstveni prispevek na konferenci
	COBISS.SI-ID		22951207
3.	Naslov	*SLO*	
		ANG	

	Opis	SLO	
		ANG	
	Šifra		
	Objavljeno v		
	Tipologija		
	COBISS.SI-ID		
4.	Naslov	SLO	
		ANG	
	Opis	SLO	
		ANG	
	Šifra		
	Objavljeno v		
	Tipologija		
	COBISS.SI-ID		
5.	Naslov	SLO	
		ANG	
	Opis	SLO	
		ANG	
	Šifra		
	Objavljeno v		
	Tipologija		
	COBISS.SI-ID		

8. Drugi pomembni rezultati projetne skupine[8]

Akreditacija pri Slovenski akreditaciji (LP-022, SIST EN ISO / IEC 17 025): Laboratorij za tekočinskoscintilacijsko spektrometrijo, (od 2008),

Prva sistematična baza podatkov za tritij v slovenskih podzemnih vodah, kar je nujna in nepogrešljiva osnova za datiranje vod in določitev ranljivosti.

Razvoj in vpeljava metod za določevanje drugih radionuklidov v vodah s tekočinskoscintilacijsko spektrometrijo:
- meritve celokupnih sevalcev alfa in beta v vzorcih vode
- določevanje Ra-226 in Ra-228 v vzorcih vode

Dosežek bo objavljen v okviru diplomskih nalog Tine Vodopivec in Maruše Jerina. Metodi bosta vključeni v študij podzemnih vod.

9. Pomen raziskovalnih rezultatov projektne skupine[9]

9.1. Pomen za razvoj znanosti[10]

SLO

Interpretacija merskih rezultatov v bližini detekcijske meje v spektrometriji gama še ni zadovoljivo rešena. V okviru projekta smo izpopolnili interpretacijo rezultatov s pomočjo Bayesianske statistike in z izdelavo empiričnega postopka, pri katerem lahko določimo verjetnosti za zmotno identifikacijo radionuklidov. Delo o sistematskih vplivih na rezultate v bližini detekcijske meje je v pripravi.

Meritve Ra-226 pri nizkih koncentracijah predstavljajo poseben problem, zaradi časovno spremenljivega ozadja. Dve deli, ki obravnavata vire ozadja radonovih potomcev v spektrometrih gama, sta poslani v objavo.

Izdelana metodologija je ustrezna za meritve pitnih vod skladno s priporočili Evropske komisije za vse sevalce gama. Za določitev geohidrokemijskih pogojev v vodonosnikih je treba metodologijo izpopolniti. Pokazalo se je, da so koncentracije torijevih izotopov, razen Th-228 pod detekcijsko mejo. Zato je potreba po novi merski tehniki s tekočinsko scintilacijsko spektrometrijo izotopov torija: tekočinskoscintilacijsko štetje alfa in beta po separaciji torija ter določanje koncentracij njegovih izotopov iz časovne odvisnosti obeh štetij.

Izboljšava metode za določevanje vsebnosti tritija po elektrolitski obogatitvi bo omogočila natančnejše datiranje podzemnih vod širom po svetu. Zmanjšanje merskih negotovosti bodo ključenega pomena že v bližnji prihodnosti, saj si pri datiranju podzemnih vod ne bomo mogli več pomagati s tritijem, izpuščenim v ozračje med jedrskimi poskusi, ki smo ga zadnjih petdeset let uspešno uporabljali kot uro. Datiranje bo odvisno od tritija, ki v naravnih procesih nastaja v vrhnjih plasteh ozračja, ki pa ga je bistveno manj kot je bilo antropogenega »bombnega« tritija. Izboljšava metode je zato ključnega pomena.

ANG

The interpretation of measurement results in the vicinity of the detection limit in gamma-ray spectrometry is not satisfactory elaborated yet. In the framework of the project we have improved the interpretation of the results by use of the Bayesian statistics and by elaboration of an empirical procedure for determination of the probability for Type I errors in radionuclide detection. A manuscript dealing with systematic influences on results near the detection limit is in preparation.

Measurements of Ra-226 near the detection limit present an additional problem because of the time variance of the spectrometer background. Two manuscripts, dealing with the radon-induced background of gamma-ray spectrometers, are sent for publication.

The methodology elaborated suffices for drinking water measurements, complying with the recommendations of the European Commission for gamma-ray emitters. For the determination of hydrogeochemical conditions in aquifers the methodology has too be improved. The concentrations of thorium isotopes, except Th-228, are below the detection limit. For these isotopes a new measurement technique is required: liquid scintillation alpha and beta counting after thorium separation and determination of its isotopes from the time dependence of both count rates.

Improvement of the method for determination of tritium content after electrolytic enrichment will enable more accurate dating of groundwater all over the world. Diminishing of measurement uncertainties will be of cruicial importance in very near future, because the amounts of tritium, released during bomb testing, practically are not detectable in the athmosphere and thereforcan't be used as a clock any more. Water age determination will be based on naturally produced tritium in the upper layers of the atmosphere, whith quantities, which are much smaller than were the quantities of antropogenic »bombing« tritium. The improvement of the method is therefore cruicial.

9.2. Pomen za razvoj Slovenije[11]

SLO

V okviru projekta zbrani in izmerjeni podatki za slovenske podzemne vode so prvi te vrste. Sistematični nabor podatkov za vse pomembnejše vodonosnike je nujno potrebna osnova za kakršnokoli datiranje slovenskih podzemnih vod. Določitev starosti podzemnih vod je ključnega pomena za opredelitev ranljivosti vod in razumevanje dinamike v vodonosnikih, kar so nepogrešljivi podatki za sonaravno gospodarjenje z enim najpomembnejših strateških virov države.

Naš prispevek je boljše poznavanje naravnega stanja slovenskih podzemnih vod, ki bo lahko v prihodnje tudi v pomoč strateškim odločitvam na področju opravljanja s pitnimi vodami. Poleg tega bomo podali tudi detajlno interpretacijo radionuklidov v podzemni vodi in v kakšnem obsegu so korelirani glede na ostale parametre vodonosnika. Opredelili bomo tudi njihov izvor, bodisi naraven ali antropogen.

ANG

This is the most comprehensive investigation of natural radioactivity of ground water in Slovenia till now. Systematic set of data for all most important aquifers is the indispensable basis for dating of slovenian groundwaters. Deteremination of groundwater age is cruicial for assesment of water vulnerability and sustainable management with one of the most important strategic source of the state.

Our contribution is better understanding of the state of ground waters in Slovenia, which is aimed to support strategic decisions in the field of ground water management. In addition a detailed interpretation of radionuclide concentration in ground water will be given, relating with other parameters of the aquifers.

10. Samo za aplikativne projekte!
Označite, katerega od navedenih ciljev ste si zastavili pri aplikativnem projektu, katere konkretne rezultate ste dosegli in v kakšni meri so doseženi rezultati uporabljeni

Cilj		
F.01	**Pridobitev novih praktičnih znanj, informacij in veščin**	
	Zastavljen cilj	○ DA ○ NE
	Rezultat	
	Uporaba rezultatov	
F.02	**Pridobitev novih znanstvenih spoznanj**	
	Zastavljen cilj	○ DA ○ NE
	Rezultat	
	Uporaba rezultatov	
F.03	**Večja usposobljenost raziskovalno-razvojnega osebja**	
	Zastavljen cilj	○ DA ○ NE
	Rezultat	
	Uporaba rezultatov	
F.04	**Dvig tehnološke ravni**	
	Zastavljen cilj	○ DA ○ NE
	Rezultat	
	Uporaba rezultatov	
F.05	**Sposobnost za začetek novega tehnološkega razvoja**	
	Zastavljen cilj	○ DA ○ NE
	Rezultat	
	Uporaba rezultatov	
F.06	**Razvoj novega izdelka**	
	Zastavljen cilj	○ DA ○ NE
	Rezultat	
	Uporaba rezultatov	
F.07	**Izboljšanje obstoječega izdelka**	
	Zastavljen cilj	○ DA ○ NE
	Rezultat	
	Uporaba rezultatov	
F.08	**Razvoj in izdelava prototipa**	
	Zastavljen cilj	○ DA ○ NE
	Rezultat	
	Uporaba rezultatov	

F.09	**Razvoj novega tehnološkega procesa oz. tehnologije**	
	Zastavljen cilj	○ DA ○ NE
	Rezultat	
	Uporaba rezultatov	
F.10	**Izboljšanje obstoječega tehnološkega procesa oz. tehnologije**	
	Zastavljen cilj	○ DA ○ NE
	Rezultat	
	Uporaba rezultatov	
F.11	**Razvoj nove storitve**	
	Zastavljen cilj	○ DA ○ NE
	Rezultat	
	Uporaba rezultatov	
F.12	**Izboljšanje obstoječe storitve**	
	Zastavljen cilj	○ DA ○ NE
	Rezultat	
	Uporaba rezultatov	
F.13	**Razvoj novih proizvodnih metod in instrumentov oz. proizvodnih procesov**	
	Zastavljen cilj	○ DA ○ NE
	Rezultat	
	Uporaba rezultatov	
F.14	**Izboljšanje obstoječih proizvodnih metod in instrumentov oz. proizvodnih procesov**	
	Zastavljen cilj	○ DA ○ NE
	Rezultat	
	Uporaba rezultatov	
F.15	**Razvoj novega informacijskega sistema/podatkovnih baz**	
	Zastavljen cilj	○ DA ○ NE
	Rezultat	
	Uporaba rezultatov	
F.16	**Izboljšanje obstoječega informacijskega sistema/podatkovnih baz**	
	Zastavljen cilj	○ DA ○ NE
	Rezultat	
	Uporaba rezultatov	
F.17	**Prenos obstoječih tehnologij, znanj, metod in postopkov v prakso**	
	Zastavljen cilj	○ DA ○ NE
	Rezultat	
	Uporaba rezultatov	
F.18	**Posredovanje novih znanj neposrednim uporabnikom (seminarji, forumi, konference)**	

	Zastavljen cilj	○ DA ○ NE
	Rezultat	
	Uporaba rezultatov	
F.19	**Znanje, ki vodi k ustanovitvi novega podjetja ("spin off")**	
	Zastavljen cilj	○ DA ○ NE
	Rezultat	
	Uporaba rezultatov	
F.20	**Ustanovitev novega podjetja ("spin off")**	
	Zastavljen cilj	○ DA ○ NE
	Rezultat	
	Uporaba rezultatov	
F.21	**Razvoj novih zdravstvenih/diagnostičnih metod/postopkov**	
	Zastavljen cilj	○ DA ○ NE
	Rezultat	
	Uporaba rezultatov	
F.22	**Izboljšanje obstoječih zdravstvenih/diagnostičnih metod/postopkov**	
	Zastavljen cilj	○ DA ○ NE
	Rezultat	
	Uporaba rezultatov	
F.23	**Razvoj novih sistemskih, normativnih, programskih in metodoloških rešitev**	
	Zastavljen cilj	○ DA ○ NE
	Rezultat	
	Uporaba rezultatov	
F.24	**Izboljšanje obstoječih sistemskih, normativnih, programskih in metodoloških rešitev**	
	Zastavljen cilj	○ DA ○ NE
	Rezultat	
	Uporaba rezultatov	
F.25	**Razvoj novih organizacijskih in upravljavskih rešitev**	
	Zastavljen cilj	○ DA ○ NE
	Rezultat	
	Uporaba rezultatov	
F.26	**Izboljšanje obstoječih organizacijskih in upravljavskih rešitev**	
	Zastavljen cilj	○ DA ○ NE
	Rezultat	
	Uporaba rezultatov	
F.27	**Prispevek k ohranjanju/varovanje naravne in kulturne dediščine**	
	Zastavljen cilj	○ DA ○ NE
	Rezultat	

	Uporaba rezultatov	
F.28	**Priprava/organizacija razstave**	
	Zastavljen cilj	○ DA ○ NE
	Rezultat	
	Uporaba rezultatov	
F.29	**Prispevek k razvoju nacionalne kulturne identitete**	
	Zastavljen cilj	○ DA ○ NE
	Rezultat	
	Uporaba rezultatov	
F.30	**Strokovna ocena stanja**	
	Zastavljen cilj	○ DA ○ NE
	Rezultat	
	Uporaba rezultatov	
F.31	**Razvoj standardov**	
	Zastavljen cilj	○ DA ○ NE
	Rezultat	
	Uporaba rezultatov	
F.32	**Mednarodni patent**	
	Zastavljen cilj	○ DA ○ NE
	Rezultat	
	Uporaba rezultatov	
F.33	**Patent v Sloveniji**	
	Zastavljen cilj	○ DA ○ NE
	Rezultat	
	Uporaba rezultatov	
F.34	**Svetovalna dejavnost**	
	Zastavljen cilj	○ DA ○ NE
	Rezultat	
	Uporaba rezultatov	
F.35	**Drugo**	
	Zastavljen cilj	○ DA ○ NE
	Rezultat	
	Uporaba rezultatov	

Komentar

11. Samo za aplikativne projekte!
Označite potencialne vplive oziroma učinke vaših rezultatov na navedena področja

	Vpliv	**Ni vpliva**	**Majhen vpliv**	**Srednji vpliv**	**Velik vpliv**	
G.01	**Razvoj visoko-šolskega izobraževanja**					
G.01.01.	Razvoj dodiplomskega izobraževanja	○	○	○	○	
G.01.02.	Razvoj podiplomskega izobraževanja	○	○	○	○	
G.01.03.	Drugo:	○	○	○	○	
G.02	**Gospodarski razvoj**					
G.02.01	Razširitev ponudbe novih izdelkov/storitev na trgu	○	○	○	○	
G.02.02.	Širitev obstoječih trgov	○	○	○	○	
G.02.03.	Znižanje stroškov proizvodnje	○	○	○	○	
G.02.04.	Zmanjšanje porabe materialov in energije	○	○	○	○	
G.02.05.	Razširitev področja dejavnosti	○	○	○	○	
G.02.06.	Večja konkurenčna sposobnost	○	○	○	○	
G.02.07.	Večji delež izvoza	○	○	○	○	
G.02.08.	Povečanje dobička	○	○	○	○	
G.02.09.	Nova delovna mesta	○	○	○	○	
G.02.10.	Dvig izobrazbene strukture zaposlenih	○	○	○	○	
G.02.11.	Nov investicijski zagon	○	○	○	○	
G.02.12.	Drugo:	○	○	○	○	
G.03	**Tehnološki razvoj**					
G.03.01.	Tehnološka razširitev/posodobitev dejavnosti	○	○	○	○	
G.03.02.	Tehnološko prestrukturiranje dejavnosti	○	○	○	○	
G.03.03.	Uvajanje novih tehnologij	○	○	○	○	
G.03.04.	Drugo:	○	○	○	○	
G.04	**Družbeni razvoj**					
G.04.01	Dvig kvalitete življenja	○	○	○	○	
G.04.02.	Izboljšanje vodenja in upravljanja	○	○	○	○	
G.04.03.	Izboljšanje delovanja administracije in javne uprave	○	○	○	○	
G.04.04.	Razvoj socialnih dejavnosti	○	○	○	○	
G.04.05.	Razvoj civilne družbe	○	○	○	○	
G.04.06.	Drugo:	○	○	○	○	
G.05.	**Ohranjanje in razvoj nacionalne naravne in kulturne dediščine in identitete**	○	○	○	○	
G.06.	**Varovanje okolja in trajnostni razvoj**	○	○	○	○	
G.07	**Razvoj družbene infrastrukture**					
G.07.01.	Informacijsko-komunikacijska infrastruktura	○	○	○	○	
G.07.02.	Prometna infrastruktura	○	○	○	○	

G.07.03.	Energetska infrastruktura		○	○	○	○	
G.07.04.	Drugo:		○	○	○	○	
G.08.	**Varovanje zdravja in razvoj zdravstvenega varstva**		○	○	○	○	
G.09.	**Drugo:**		○	○	○	○	

Komentar

12. Pomen raziskovanja za sofinancerje, navedene v 2. točki [12]

1.	**Sofinancer**		
	Vrednost sofinanciranja za celotno obdobje trajanja projekta je znašala:		**EUR**
	Odstotek od utemeljenih stroškov projekta:		**%**
	Najpomembnejši rezultati raziskovanja za sofinancerja		**Šifra**
	1.		
	2.		
	3.		
	4.		
	5.		
	Komentar		
	Ocena		
2.	**Sofinancer**		
	Vrednost sofinanciranja za celotno obdobje trajanja projekta je znašala:		**EUR**
	Odstotek od utemeljenih stroškov projekta:		**%**
	Najpomembnejši rezultati raziskovanja za sofinancerja		**Šifra**
	1.		
	2.		
	3.		
	4.		
	5.		
	Komentar		
	Ocena		

3.	**Sofinancer**			
	Vrednost sofinanciranja za celotno obdobje trajanja projekta je znašala:			**EUR**
	Odstotek od utemeljenih stroškov projekta:			**%**
	Najpomembnejši rezultati raziskovanja za sofinancerja			**Šifra**
		1.		
		2.		
		3.		
		4.		
		5.		
	Komentar			
	Ocena			

C. IZJAVE

Podpisani izjavljam/o, da:

- so vsi podatki, ki jih navajamo v poročilu, resnični in točni
- se strinjamo z obdelavo podatkov v skladu z zakonodajo o varstvu osebnih podatkov za potrebe ocenjevanja, za objavo 6., 7. in 8. točke na spletni strani http://sicris.izum.si/ ter obdelavo teh podatkov za evidence ARRS
- so vsi podatki v obrazcu v elektronski obliki identični podatkom v obrazcu v pisni obliki
- so z vsebino zaključnega poročila seznanjeni in se strinjajo vsi soizvajalci projekta

Podpisi:

Matjaž Aleš Korun	in	
podpis vodje raziskovalnega projekta		zastopnik oz. pooblaščena oseba RO

Kraj in datum: Ljubljana 19.4.2011

Oznaka poročila: ARRS-RPROJ-ZP-2011-1/57

---

[1] Zaradi spremembe klasifikacije družbeno ekonomskih ciljev je potrebno v poročilu opredeliti družbeno ekonomski cilj po novi klasifikaciji. Nazaj

[2] Samo za aplikativne projekte. Nazaj

[3] Napišite kratko vsebinsko poročilo, kjer boste predstavili raziskovalno hipotezo in opis raziskovanja. Navedite ključne ugotovitve, znanstvena spoznanja ter rezultate in učinke raziskovalnega projekta. Največ 18.000 znakov vključno s presledki (približno tri strani, velikosti pisave 11). Nazaj

[4] Realizacija raziskovalne hipoteze. Največ 3.000 znakov vključno s presledki (približno pol strani, velikosti pisave 11). Nazaj

[5] V primeru bistvenih odstopanj in sprememb od predvidenega programa raziskovalnega projekta, kot je bil zapisan v predlogu raziskovalnega projekta oziroma v primeru sprememb, povečanja ali zmanjšanja sestave projektne skupine v zadnjem letu izvajanja projekta (obrazložitev). V primeru, da sprememb ni bilo, to navedite. Največ 6.000 znakov vključno s presledki (približno ena stran, velikosti pisave 11). Nazaj

[6] Navedite največ pet najpomembnejših znanstvenih rezultatov projektne skupine, ki so nastali v času trajanja projekta v okviru raziskovalnega projekta, ki je predmet poročanja. Za vsak rezultat navedite naslov v slovenskem in angleškem jeziku (največ 150 znakov vključno s presledki), rezultat opišite (največ 600 znakov vključno s presledki) v slovenskem in angleškem jeziku, navedite, kje je objavljen (največ 500 znakov vključno s presledki), izberite ustrezno šifro tipa objave po Tipologiji dokumentov/del za vodenje bibliografij v sistemu COBISS ter napišite ustrezno COBISS.SI-ID številko bibliografske enote.
Navedeni rezultati bodo objavljeni na spletni strani http://sicris.izum.si/.

PRIMER (v slovenskem jeziku):
Naslov: Regulacija delovanja beta-2 integrinskih receptorjev s katepsinom X;
Opis: Cisteinske proteaze imajo pomembno vlogo pri nastanku in napredovanju raka. Zadnje študije kažejo njihovo povezanost s procesi celičnega signaliziranja in imunskega odziva. V tem znanstvenem članku smo prvi dokazali… (največ 600 znakov vključno s presledki)
Objavljeno v: OBERMAJER, N., PREMZL, A., ZAVAŠNIK-BERGANT, T., TURK, B., KOS, J.. Carboxypeptidase cathepsin X mediates ß2 - integrin dependent adhesion of differentiated U-937 cells. Exp. Cell Res., 2006, 312, 2515-2527, JCR IF (2005): 4.148
Tipopologija: 1.01 - Izvirni znanstveni članek
COBISS.SI-ID: 1920113 Nazaj

[7] Navedite največ pet najpomembnejših družbeno-ekonomsko relevantnih rezultatov projektne skupine, ki so nastali v času trajanja projekta v okviru raziskovalnega projekta, ki je predmet poročanja. Za vsak rezultat navedite naslov (največ 150 znakov vključno s presledki), rezultat opišite (največ 600 znakov vključno s presledki), izberite ustrezen rezultat, ki je v Šifrantu raziskovalnih rezultatov in učinkov (Glej: http://www.arrs.gov.si/sl/gradivo/sifranti/sif-razisk-rezult.asp), navedite, kje je rezultat objavljen (največ 500 znakov vključno s presledki), izberite ustrezno šifro tipa objave po Tipologiji dokumentov/del za vodenje bibliografij v sistemu COBISS ter napišite ustrezno COBISS.SI-ID številko bibliografske enote.
Navedeni rezultati bodo objavljeni na spletni strani http://sicris.izum.si/. Nazaj

[8] Navedite rezultate raziskovalnega projekta v primeru, da katerega od rezultatov ni mogoče navesti v točkah 6 in 7 (npr. ker se ga v sistemu COBISS ne vodi). Največ 2.000 znakov vključno s presledki. Nazaj

[9] Pomen raziskovalnih rezultatov za razvoj znanosti in za razvoj Slovenije bo objavljen na spletni strani: http://sicris.izum.si/ za posamezen projekt, ki je predmet poročanja. Nazaj

[10] Največ 4.000 znakov vključno s presledki Nazaj

[11] Največ 4.000 znakov vključno s presledki Nazaj

[12] Rubrike izpolnite/prepišite skladno z obrazcem "Izjava sofinancerja" (http://www.arrs.gov.si/sl/progproj/rproj/gradivo/), ki ga mora izpolniti sofinancer. Podpisan obrazec "Izjava sofinancerja" pridobi in hrani nosilna raziskovalna organizacija – izvajalka projekta. Nazaj

Obrazec: ARRS-RPROJ-ZP/2011-1 v1.01
0C-D5-F9-4A-BC-7D-60-4B-7F-91-F9-3E-3C-03-03-9B-28-81-40-43

zap. št.	kraj vzorčevanja	datum vzorčenja	vrsta vzorca	x	y
9	B-2 Brestovica	22.10.2008 11:47	vodnjak	74730	392755
10	B-3 Brestovica	22.10.2008 13:28	piezometer	74700	392400
8	B-9 Brestovica	21.10.2008 16:00	vodnjak	75106	392109
56	B-9 Brestovica	11.6.2009 14:41	vrtina	75106	392109
78	B-9 Brestovica	09.10.2009 16:00	vodnjak	75106	392109
22	BLP-2/04	15.4.2009 16:07	piezometer	162986	602609
32	BLP-2/04	13.5.2009 00:00	piezometer	162986	602609
121	BLP-2/04	28.4.2010 16:04	piezometer	162986	602609
61	Bočič	14.7.2009 10:57	izvir	131174,6	383899,6
73	Bočič	07.10.2009 11:34	izvir	131174,6	383899,6
125	Bohinjska Bistrica	09.6.2010 11:49	izvir	124151	417456
174	Bohinjska Bistrica	15.10.2010 12:15	izvir	124151	417456
62	Boka	14.7.2009 11:30	izvir	131727,6	384231,6
74	Boka	07.10.2009 12:01	izvir	131727,6	384231,6
42	C-4 Domžale	19.5.2009 09:34	vrtina	111465	467594
122	C-4 Domžale	29.4.2010 10:04	vrtina	111465	467594
127	Črna Logarska dolina	10.6.2010 12:23	izvir	140580	472369
168	Črna Logarska dolina	13.10.2010 12:28	izvir	140580	472369
49	DAC-3/98	26.5.2009 13:34	vodnjak	85100	541049
108	DAC-3/98	16.11.2009 17:15	piezometer	85100	541049
158	DAC-3/98	03.8.2010 10:12	piezometer	85100	541049
129	Debelčev mlin	10.6.2010 16:00	izvir	123199	472078
187	Debelčev mlin	15.11.2010 13:45	izvir	123199	472078
20	DEV-1	15.4.2009 11:20	vodnjak	150900	569790
101	DEV-1	12.11.2009 10:40	vodnjak	150900	569790
130	Dobličica	29.6.2010 11:46	izvir	45265	511576
179	Dobličica	28.10.2010 10:55	izvir	45265	511576
126	Dobravca	09.6.2010 13:48	izvir	136627	433366
166	Dobravca	12.10.2010 12:25	izvir	136627	433366
44	Dobrova-Jablance	19.5.2009 14:02	izvir	100633	535519
107	Dobrova-Jablance	16.11.2009 15:45	izvir	100633	535519
150	Framski slap	22.7.2010 11:32	zajetje	150827	542541
186	Framski slap	15.11.2010 11:15	izvir	150827	542541
64	Glijun	14.7.2009 13:00	izvir	133400	385700
76	Glijun	07.10.2009 14:05	izvir	133400	385700
149	Gornji Ig	21.7.2010 14:42	izvir	86400	461000
177	Gornji Ig	27.10.2010 12:30	izvir	86400	461000
37	Gornji Lakoš	14.5.2009 15:08	vodnjak	157701	608756
134	Grad Snežnik	30.6.2010 13:42	izvir	59911	459004
189	Grad Snežnik	15.11.2010 10:45	izvir	59911	459004
34	Grad-1/02	13.5.2009 13:14	vrtina	184938	583441
119	Grad-1/02	28.4.2010 11:44	vrtina	184938	583441
151	Gradišče	22.7.2010 13:29	zajeti izvir	167521	584972
171	Gradišče	14.10.2010 13:30	zajeti izvir	167521	584972
143	Grajsko zajetje	15.7.2010 10:29	izvir	102738	446793
188	Grajsko zajetje	15.11.2010 15:25	izvir	102738	446793
45	Grešnikov hrib	20.5.2009 10:19	izvir	99250	473230
118	Grešnikov hrib	07.12.2009 14:05	izvir	99250	473230
29	Hotešk	12.5.2009 13:01	izvir	110160	406612

94	Hotešk	28.10.2009 11:28	izvir	110160	406612
27	Hubelj	11.5.2009 13:43	izvir	85022	416048
95	Hubelj	28.10.2009 13:15	izvir	85022	416048
58	Ilirska Bistrica	16.6.2009 10:49	izvir	47345	441976
97	Ilirska Bistrica	29.10.2009 10:00	izvir	47345	441976
144	Iščica	15.7.2010 12:13	izvir	90597	463736
184	Iščica	29.10.2010 12:17	izvir	90597	463736
137	Izvir Soče	12.7.2010 16:36	izvir	141700	402200
175	Izvir Soče	15.10.2010 14:15	izvir	141700	402200
23	Jelševa Loka	16.4.2009 11:18	izvir	136200	522000
89	Jelševa Loka	27.10.2009 11:30	izvir	136200	522000
48	Jurčičev izvir	25.5.2009 16:19	izvir	111215	454084
123	Jurčičev izvir	29.4.2010 12:14	izvir	111215	454084
68	Kamniška Bistrica	15.7.2009 14:30	izvir	131580	468815
88	Kamniška Bistrica	21.10.2009 15:30	izvir	131580	468815
153	Kamniška Bistrica	27.7.2010 08:20	izvir	131580	468815
14	Kleče	24.2.2009 09:40	lizimeter		
65	Krajcarica	14.7.2009 16:30	izvir	138350	406100
77	Krajcarica	07.10.2009 15:32	izvir	138350	406100
18	Krka	09.4.2009 13:55	izvir	82860	482630
109	Krka	17.11.2009 10:30	izvir	82860	482630
154	Krka	27.7.2010 09:50	izvir	82860	482630
69	Kropa	15.7.2009 16:00	izvir	127445	487875
92	Kropa	27.10.2009 16:40	izvir	127445	487875
15	Krupa	08.4.2009 13:36	izvir	54532	517307
114	Krupa	18.11.2009 14:03	izvir	54532	517307
157	Krupa	02.8.2010 11:45	izvir	54532	517307
66	Lipnica	14.7.2009 18:45	izvir	131090	435700
87	Lipnica	21.10.2009 13:50	izvir	131090	435700
145	Lipnik	20.7.2010 10:25	izvir	138300	425500
165	Lipnik	12.10.2010 11:30	izvir	138300	425500
38	Lipovci 2271	14.5.2009 16:48	vrtina	165177	594133
25	LMP-1/06	06.5.2009 14:18	vrtina	103755	461963
124	LMP-1/06	29.4.2010 13:04	vodnjak	103755	461963
128	Lučnica	10.6.2010 13:43	izvir	129972	477111
167	Lučnica	13.10.2010 10:30	izvir	129972	477111
11	Mahniči	19.11.2008 12:00	izvir	71156	415345
30	Malenščica	12.5.2009 15:27	izvir	75609	442532
116	Malenščica	07.12.2009 11:30	izvir	75609	442532
140	Mazej	13.7.2010 14:29	izvir	141328	500219
169	Mazej	13.10.2010 13:48	izvir	141328	500219
131	Metliški Obrh	29.6.2010 13:05	izvir	56485	525155
180	Metliški Obrh	28.10.2010 11:20	izvir	56485	525155
3	Miren 0330	13.10.2008 15:34	vodnjak	84800	392520
52	Miren 0330	02.6.2009 16:12	vodnjak	84800	392520
81	Miren 0330	19.10.2009 17:25	vodnjak	84800	392520
43	Mitovšek	19.5.2009 12:10	izvir	108450	502720
112	Mitovšek	18.11.2009 10:23	izvir	108450	502720
31	Močilnik	12.5.2009 16:57	izvir	90240	445550
117	Močilnik	07.12.2009 13:10	izvir	90240	445550
146	Mošenik	20.7.2010 13:28	izvir	142100	444273

164	Mošenik	12.10.2010 09:10	izvir	142100	444273
135	Mrzlek	12.7.2010 10:43	izvir	95415	395150
172	Mrzlek	15.10.2010 10:20	izvir	95415	395150
4	NG-4/75	14.10.2008 13:30	piezometer	84377	391735
50	NG-4/75	02.6.2009 12:37	vrtina	84377	391735
82	NG-4/75	20.10.2009 12:02	vrtina	84377	391735
60	O-1/91	18.6.2009 14:04	vrtina	48273	410870
80	O-1/91	19.10.2009 14:15	vrtina	48273	410870
141	Obrh Rinža	14.7.2010 10:50	izvir	58000	486700
190	Obrh Rinža	25.11.2010 10:00	izvir	58000	486700
59	Odolina	16.6.2009 12:09	izvir	50062	423852
98	Odolina	29.10.2009 11:05	izvir	50062	423852
1	Orehovlje 0420	13.10.2008 12:00	vodnjak	83546	392740
51	Orehovlje 0420	02.6.2009 14:17	vodnjak	83546	392740
83	Orehovlje 0420	20.10.2009 15:03	vodnjak	83546	392740
40	OV-29	18.5.2009 15:32	hišni vodnj	143716	556716
103	OV-29	12.11.2009 14:50	hišni vodnj	143716	556716
161	OV-29	12.8.2010 14:30	hišni vodnj	143716	556716
142	Padiščak	14.7.2010 14:03	izvir	39614	397009
185	Padiščak	15.11.2010 13:15	izvir	39614	397009
72	Pasji rep	22.7.2009 10:00	izvir	71535	420148
100	Pasji rep	29.10.2009 14:00	izvir	71535	420148
6	Pliskovica P-1	21.10.2008 11:00	vrtina	69843	405820
28	Podroteja	11.5.2009 15:08	izvir	94000	425180
93	Podroteja	28.10.2009 10:10	izvir	94000	425180
133	Podturn	30.6.2010 11:30	izvir	66422	503457
191	Podturn	25.11.2010 11:40	izvir	66422	503457
46	Potok pri dvorcu Visoko	20.5.2009 13:09	površinski	109652	438992
105	Potok pri dvorcu Visoko	13.11.2009 10:50	površinski	109652	438992
147	Pšata	20.7.2010 14:38	izvir	124201	462272
183	Pšata	29.10.2010 10:15	izvir	124201	462272
19	Rakitnica	10.4.2009 11:00	izvir	61215	480436
110	Rakitnica	17.11.2009 12:15	izvir	61215	480436
39	Rankovci 3370	18.5.2009 13:52	vrtina	170605	583057
53	Rižana	03.6.2009 11:24	izvir	43209	413333
99	Rižana	29.10.2009 12:30	izvir	43209	413333
156	Rižana	27.7.2010 11:42	izvir	43209	413333
12	Rv-2/90	19.11.2008 12:00	vrtina	71140	415325
57	Rv-2/90	15.6.2009 11:40	vrtina	71140	415325
79	Rv-2/90	15.10.2009 10:55	vrtina	71140	415325
13	Rv-3/90	19.11.2008 12:00	vrtina	69962	416358
67	Savica	15.7.2009 10:20	izvir	128350	407330
86	Savica	21.10.2009 11:45	izvir	128350	407330
160	Savica	12.8.2010 10:25	izvir	128350	407330
139	Skorba	13.7.2010 12:41	vrtina	141953	563379
170	Skorba	14.10.2010 11:31	vrtina	141953	563379
16	Ščetar	08.4.2009 16:16	izvir	87015	523032
113	Ščetar	18.11.2009 12:10	izvir	87015	523032
5	ŠE-1/94	16.10.2008 12:00	vrtina	87285	394310
55	ŠE-1/94	03.6.2009 17:47	vrtina	87285	394310
85	ŠE-1/94	20.10.2009 18:02	vrtina	87285	394310

54	Šempeter 0220	03.6.2009 16:17	vrtina	87520	394940
84	Šempeter 0220	20.10.2009 16:37	vodnjak	87520	394940
2	Šempeter 0840	13.10.2008 14:08	hišni vodnja	123490	510688
41	Šempeter 0840	18.5.2009 17:48	hišni vodnja	123490	510688
115	Šempeter 0840	19.11.2009 14:30	hišni vodnja	123490	510688
159	Šempeter 0840	03.8.2010 16:03	hišni vodnja	123490	510688
71	Šumec 1	16.7.2009 15:20	izvir	152600	487310
91	Šumec 1	27.10.2009 14:40	izvir	152600	487310
132	Težka voda	29.6.2010 14:50	izvir	69141	516536
181	Težka voda	28.10.2010 13:40	izvir	69141	516536
17	Tominčev izvir	09.4.2009 00:00	izvir	72369	498020
111	Tominčev izvir	17.11.2009 13:55	izvir	72369	498020
47	Trebija	20.5.2009 14:19	izvir	106590	430333
104	Trebija	13.11.2009 10:10	izvir	106590	430333
7	VB-4/80, črpališče Klariči	21.10.2008 14:17	vodnjak	75343	391455
24	Velika Toplica	16.4.2009 13:17	izvir	128320	545040
106	Velika Toplica	16.11.2009 12:20	izvir	128320	545040
36	Veščica 0120	14.5.2009 13:42	vrtina	154648	596753
148	VG-10 Mala Goba	21.7.2010 10:27	vrtina	99601	498990
178	VG-10 Mala Goba	27.10.2010 14:55	vrtina	99601	498990
26	Vipava	11.5.2009 12:29	izvir	78321	419945
96	Vipava	28.10.2009 14:25	izvir	78321	419945
155	Vipava	27.7.2010 13:00	izvir	78321	419945
152	Vodice Vo-1	23.7.2010 08:14	vrtina	116160	462653
182	Vodice Vo-1	29.10.2010 09:25	vrtina	116160	462653
33	VP-1/2000	13.5.2009 00:00	vrtina	178100	600250
120	VP-1/2000	28.4.2010 13:24	vrtina	178100	600250
138	Vt-1 Tinsko	13.7.2010 11:03	vrtina	113876	541943
176	Vt-1 Tinsko	27.10.2010 09:40	vrtina	113876	541943
35	Vučja vas	14.5.2009 10:34	vrtina	162220	584566
21	Vurberk	15.4.2009 12:57	izvir	149665	562240
102	Vurberk	12.11.2009 12:25	izvir	149665	562240
136	Zadlaščica	12.7.2010 14:15	izvir	121490	406210
173	Zadlaščica	15.10.2010 12:12	izvir	121490	406210
70	Žegnan studenec	16.7.2009 12:52	izvir	149185	518038
90	Žegnan studenec	27.10.2009 12:50	izvir	149185	518038
63	Žvika	14.7.2009 12:09	izvir	131956	384853,6
75	Žvika	07.10.2009 12:28	izvir	131956	384853,6
162		24.6.2010 12:00	deževnica		
163		09.8.2010 12:00	deževnica		

z	^{3}H	Δ ^{3}H	MDC	^{210}Pb	Δ ^{210}Pb	^{228}Th	Δ ^{228}Th	^{40}K
36	474	100						
41	743	130						
22	632	85						
22	553	73		15,78	0,87	0,10	0,05	22,26
22	673	95		13,66	1,35			21,76
158	1108	147		8,78	0,72	0,33	0,13	43,40
158	1208	110						
158	1035	101						
351	735	47						
351	566	79						
	702	58						
377,6	793	144						
377,6	856	80						
305	0	35	58	4,91	0,52	0,10	0,07	31,33
305	527	44						
	705	51						
464	967	99		5,02	0,90			59,05
464	942	82		3,69	0,99			64,66
464								
	622	47						
255	149	49		3,61	0,58	0,82	0,09	28,22
255	117	14		5,93	0,71			25,90
461	699	53						
410	855	78		4,39	0,79			22,66
410	628	55		4,30	0,61			25,52
435	813	64		1,26	0,26	0,26	0,07	1,73
435	707	54		3,80	0,62			2,79
165	524	79						
271	91	18		4,71	0,67			31,31
271	171	18						
335	690	98		8,62	0,50	0,95	0,08	18,22
335	851	187		2,18	0,41			11,54
190	585	86		0,89	0,40			6,80

190	800	65	1,13	0,38			9,80
225	661	79	2,62	0,55			4,01
225	891	77	2,90	0,43			4,08
420	262	50	3,82	0,40	0,06	0,05	6,02
420	544	49	2,63	0,47			5,88
420	787	101	2,44	0,62	0,10	0,08	12,78
420	719	59	10,24	1,33			15,05
327	590	59	1,56	0,75			19,81
327	742	58					
600	869	62	0,98	0,24	0,08	0,05	2,19
600	715	65	1,38	0,38			1,65
600							
	867	78					
690	982	58	1,83	0,39			2,37
690	697	84	0,00	0,73			2,76
270	665	65	4,78	0,50	0,26	0,07	26,27
270	209	31	3,41	0,58			33,17
270							
406	739	62	4,07	0,40	0,10	0,05	6,26
406	742	91	1,96	0,48			7,02
136	849	130	32,75	2,04			14,46
136	867	85	7,65	0,87			24,46
136							
492	762	120	1,09	0,33	0,23	0,07	5,24
492	721	52	2,97	0,42			5,52
181	876	79	9,74	1,05			57,94
314	740	78	5,03	0,65	0,08	0,07	16,87
314	826	57					
	603	44					
255	958	129					
459	695	75	3,66	0,47	0,03	0,06	9,64
459	664	65	5,43	0,68			9,19
55	655	93					
55	406	73	1,34	0,42	0,09	0,06	47,47
55	732	81	1,97	0,75			61,32
270	705	178	2,92	0,42	0,11	0,05	7,89
270	591	60	3,98	0,58			8,75
290	748	69	3,86	0,32	0,13	0,04	13,66
290	676	54	6,55	0,71			23,60

44	764	35						
44	501	56						
44	619	67						
27	144	29		4,07	0,67	0,09	0,07	27,78
27	0	56	92	2,77	0,68			26,80
509	564	97		1,92	0,36	0,14	0,09	25,97
509	777	114		1,19	0,37			11,25
50	642	109						
50	667	78						
50	552	53						
244	793	76		12,48	1,64			307,90
244	928	164		13,31	1,23			280,10
244								
227	657	86		1,27	0,41	0,13	0,04	3,40
227	571	68		1,00	0,43			42,94
202	1022	135						
327	593	62		6,29	0,59			6,91
327	807	72		4,66	0,59			7,41
755	586	61		2,38	0,58			16,86
755	629	65		1,15	0,40			16,72
453	562	55		9,55	0,58	0,10	0,05	7,95
453	748	65		3,97	0,51			7,22
198	753	81		21,38	1,53			43,23
72	652	99		2,44	0,38	0,12	0,05	12,19
72	492	70		4,64	0,64			15,77
72								
251	715	109						
251	423	33		4,92	0,59	0,13	0,08	16,77
251	518	57		3,46	0,61			15,86
273	1016	87						
840	756	70		0,47	0,27	0,10	0,06	1,53
840	710	76		1,04	0,48			0,00
840								
184	467	87		4,38	0,43	0,36	0,06	16,95
184	422	56		6,16	0,77			17,94
68	0	33	52					
68	563	96						
68	0	38	63					

69	632	57					
69	419	55					
272	631	63					
272	1066	97	17,69	1,42			31,60
272			15,92	1,19			30,15
272							
665	1178	85	1,15	0,26	0,22	0,05	4,50
665	1111	88	2,48	0,47			3,80
222	680	67	13,29	0,80	0,34	0,08	10,92
222	831	60	4,44	0,70			14,85
470	668	129	4,29	0,74			9,11
470	769	75	2,63	0,43			8,04
23	670	126					
284	829	109	4,21	0,57	0,06	0,06	5,84
284	653	123	1,33	0,53			5,79
172	708	86					
100	592	70	4,98	0,70			9,94
100	764	68	5,23	0,55			8,06
100							
250			4,81	0,64			21,26
250	58	11					
	228	75					
342	1189	121	2,46	0,53	0,20	0,06	19,77
342	1400	131	4,28	0,58			16,46
1490	749	47	7,42	0,50	0,10	0,05	19,48
1490	860	126	12,26	0,98			15,58
385	700	60					
385	508	47					

Δ ^{40}K	^{228}Ra	Δ ^{228}Ra	^{238}U	Δ ^{238}U	^{226}Ra	Δ ^{226}Ra
2,06	0,88	0,17	6,50	0,57	2,44	0,28
2,69						
3,49	3,05	0,23	5,29	0,14	3,39	0,31
2,52	0,24	0,15	5,12	0,36	0,41	0,13
6,58						
6,88						
2,45	5,09	0,25	16,89	1,68	3,55	0,25
3,01						
2,81						
2,98						
0,63	0,06	0,10			0,23	0,10
1,16						
3,73						
1,44	1,85	0,16	2,61	0,32	16,15	0,92
1,99						
1,53						

1,55						
1,33						
1,12						
0,97	0,44	0,17	5,29	0,14	1,11	0,15
1,60						
1,45	0,81	0,23	4,36	0,17	1,22	0,17
2,46						
2,67						
0,70	0,49	0,18			0,54	0,15
1,13						
1,06						
1,07						
2,25	0,86	0,19	4,88	0,62	0,96	0,14
3,90						
0,96	0,63	0,19			0,16	0,15
1,71						
2,49						
2,89						
0,99	0,62	0,28			0,23	0,12
1,08						
6,39						
1,58	0,59	0,18	11,11	0,28		
1,16	0,48	0,18	4,28	0,49	1,09	0,17
1,64						
3,59	0,79	0,14	5,32	0,34	0,50	0,11
6,57						
0,95	0,55	0,12	1,24	0,07	0,19	0,12
1,73						
1,20	0,60	0,12	4,21	0,07	0,68	0,09
2,76						

2,49	0,73	0,31			0,24	0,20
3,43						
2,19	0,75	0,17	3,60	0,15	0,74	0,14
1,61						
32,28						
28,67						
0,93	0,20	0,11			0,19	0,10
4,60						
1,23						
1,53						
2,20						
2,09						
1,11	0,61	0,17	4,54	0,29	1,15	0,13
1,33						
4,97						
1,28	0,67	0,14			0,81	0,15
2,07						
1,86	0,83	0,20	10,73	0,55	2,37	0,30
2,68						
0,75	0,27	0,17			0,23	0,11
2,35						
0,94	1,30	0,15	3,71	3,29	3,39	0,31
2,42						

4,02						
3,34						
0,94	0,65	0,12			2,29	0,25
1,69						
1,27	0,71	0,25	5,13	0,83	1,56	0,20
2,04						
1,70						
1,38						
1,19	0,72	0,17	3,17	0,16	4,84	0,38
1,37						
1,64						
1,41						
2,83						
1,86	1,03	0,13	13,47	0,32	0,81	0,12
2,13						
2,47	0,59	0,20			0,18	0,09
2,07						

Background of radon daughters in gamma-ray spectrometric measurements

P. Maver Modec[1*], M. Korun[1], M. Martelanc[2], B. Vodenik[1]

[1]Jožef Stefan Institute, Jamova cesta 39, Ljubljana, Slovenia
[2]Faculty of Computer and Information Science, Tržaška cesta 25, Ljubljana, Slovenia

Abstract: An analysis of radon-induced background on nine high-resolution gamma-ray spectrometers is presented. The contributions of the detector contamination, contamination of air inside the shield cavity and the radiation penetrating the detector shield are evaluated. Whereas the detector contamination and the radiation penetrating the shield are constant in time, the contamination of air varies due to variation of the outdoor temperature. The data extracted from the analysis are used for calculation of the background count rates during sample measurements and the count rates in peaks too weak to be measured directly.

Introduction.

When samples from the environment are measured on gamma-ray spectrometers ^{226}Ra can be determined either from its peak occurring at the energy 186 keV or from the concentrations of radon daughters in the sample. The later method has

---

[*] Corresponding author: Petra Maver Modec, tel.: +386 1 4773900, fax: +386 1 4773151, e-mail: petra.maver@ijs.si

the advantage that it is more sensitive. Radon daughters ^{214}Pb and ^{214}Bi radiate at several energies with the probability which is much larger than the probability for emission of the gamma-rays in the decay of ^{226}Ra. Unfortunately, the activity of ^{226}Ra in the sample is small a substantial part of the areas of peaks signaling the presence of radon daughters in the sample may originate in the spectrometer background. To arrive at an unbiased result the peak areas must be corrected for the background contribution. Therefore background measurements are performed, which are used to determine the count rates in the peaks occurring in the spectra in the absence of the sample.

Radon daughters in the spectrometer background originate in the presence of ^{226}Ra in the detector, the shielding, the materials surrounding the shielding where the rays penetrating the shield originate, and in the presence of radon and its daughters in the air filling the shield's cavity. Whereas the contribution from contamination from detector, shielding and the environment is constant in time, the contribution due to radon contamination in the air may vary. Therefore the count rate in the background peaks due to radon daughters may vary with time and can be not determined as a simple average over the count rates in repeated background measurements.

It is the purpose of this contribution to present an analysis of the radon-induced background and the sources of background due to radon daughters in the spectrometers of the Laboratory for Radiological Measuring Systems and Radioactivity Measurements at the Jožef Stefan.

Materials and Methods

The counting room is located in the basement, below the ground level. It is kept at a constant temperature. It is not ventilated to avoid possible contamination, the air is exchanged only by the draught. The draught is stronger at low outside temperatures since then the cooler air from the ambient tends to replace the warmer air in the counting room. During summer, in the counting room radon concentration may reach 600 Bq/m^3 in winter the average concentration is 70 Bq/m^3.

The counting room houses nine spectrometers with high-energy germanium detectors of various properties. The characteristics of the detector shields are given in Table 1. The graded layers to prevent registration of X-rays are omitted from the table because of clearness. The shield cavities, except the cavity f the detector PO, are flushed constantly with nitrogen in order to replace ambient air, contaminated with radon, from the interior of the shield. The nitrogen is obtained by evaporation of liquid nitrogen, aged for two weeks to allow radon to decay. Because of the limited supply of nitrogen, some shields are not flushed completely, therefore some contamination of radon daughters remains within the cavity. This is reflected in seasonal variations of the background of radon daughters in some spectrometers, which occurs in spite of flushing. The seasonal variations of the cunt rate in the peak at 352 keV in the background measurements on the spectrometer MG, having the largest shield cavity, are presented in Fig. 1. On Fig. 2 this peak count rate is presented as a function of the outside temperature, averaged over the counting time of the measurement.

Background measurements are performed at times when samples for activity measurements are not available. The acquisition time of background measurement is between 3 days and 12 days. Besides other peaks, occurring in the background spectrum, the count rate in the peaks of radon daughters is determined from the measured spectra. Some of the peaks are not identified in all background measurements because of poor statistics or poor deconvolution of multiplets when statistical uncertainties of peak areas are high. Here we analyze only the count rates at energies, where peaks are recognized in a great majority of measurements. These peaks occur at energies 75 keV, 77 keV, 87 keV, 242 keV, 295 keV, 352 keV, 609 keV, 768 keV, 1120 keV, 1238 keV, 1765 keV, 2204 keV and 2447 keV. Some of these energies are omitted from the data on spectrometers whre the peaks are not recognized in background measurements frequently enough.

Results

It can be observed on Fig. 1 that count rates in background peaks may be subject to seasonal variations. Below a critical outside temperature the count rate does not depend on the outside temperature, since then the radon concentration is low enough that the flushing effectively removes all radon from the shield cavity. The effectiveness of flushing depends on the volume of the air in the cavity, intensity of flushing and the permeability of the shield for air. On the detectors, which exhibit the temperature dependence, this critical temperature varies between 14 °C and 20 °C. The count rate below the critical temperature is determined, besides by the detector efficiency, by the contamination of the detector and shield with ^{226}Ra and by the penetration rate of gamma-rays from the counting room through the shield. Above the critical temperature the count rate increases linearly with the outside temperature. The rate at which it increases depends on the effectiveness of flushing, the volume of the shield cavity and the detector efficiency.

During the background measurements the detector measures the flux of gamma-rays at the center of the shield's cavity, where it is placed. To convert count rates into activities, characterizing contaminations, the response of the detector and the probability for emission of gamma-rays has to be taken into account. To assess the contamination, apparent activities $A(E)$ are calculated as

$$A(E) = \frac{n(E)}{\eta(E)b(E)} \qquad ,$$

where $n(E)$ denotes the count rate in the peak at the energy E, $\eta(E)$ the counting efficiency of a source, positioned at the detector surface on the symmetry axis of the detector cap, radiating gamma-rays with the energy E, and $b(E)$ the probability for emission of gamma-rays with the energy E in a decay of a radon daughter. It should be noted that the point-source efficiency only poorly represents the average probability for registration of a gamma-ray impinging under large angle on the detector cap, since it describes the probability for registration of a photon emitted isotropically from the point source. Although the point-source efficiency used is maximal, it underestimates the average probability. Therefore apparent activities overestimate flux rates, normalized to the emission probability of unity. The Fig. 3 presents apparent activities, corresponding to count rates in the spectrum below the critical temperature, for the spectrometers installed in the counting room.

Discussion

It can be observed that in the energy range above 500 keV the apparent activity increases with energy in almost all spectrometers. In general, the apparent activity is an increasing function of energy. This is due to the decreasing attenuation coefficient for photons in the shielding material. The rate of increasing bears the information on the thickness of the material between the contamination and the detector. Below 500 keV the photons can't penetrate the layers of the shielding, therefore here the apparent activity indicates the contamination of the detector and inner surface of the cavity with ^{226}Ra. The increase of the apparent activities over this level indicates contributions from the shield material and from the exterior of the shield.

The count rate in the X-ray peaks is difficult to interpret in terms of the apparent activity because of the X-ray fluorescence of lead, which interferes with the X-ray lines from ^{214}Bi, which belong to the decay of radon daughters. Namely, the graded layers (made of cadmium and copper) do not attenuate the fluorescence completely. In addition to that, deconvolution of multiplets is not reliable at large statistical uncertainties of peak areas. Therefore apparent activities at energies which coincide with the energy of lead X-rays (75 keV and 87 keV) are given only in cases where no lead is used in the shielding, or where the inner layer absorbs the fluorescent X-rays completely and where the decomposition of multiplets is reliable enough. It can be seen on the Fig. 3 that apparent activities calculated from X-ray peak reproduce roughly the apparent activities due to the detector contamination except on the detector FE, where the increased activity indicates presence of lead within the detector.

The flux of gamma-rays at the outer surface of the inner layer, $A_O(E)$, can be calculated from the increase of the apparent activity over its value, due to the contamination of the detector and the inner surface, and corrected for the attenuation of the gamma-rays in the inner layer. It is calculated as

$$A_O(E) = (A(E) - A_D)e^{\mu_I(E)d_I\rho_I} \qquad ,$$

where $\mu_I(E)$, d_I and ρ_I denote the attenuation coefficient, the thickness and the density of the material of the inner layer respectively. A_D denotes the apparent activity due to the contamination of the detector and the shield and is given by the apparent activity averaged in the energy range between 200 keV and 400 keV. This calculation can be performed for all detectors except for the detector RA, where the thickness of the shield is not well defined. The apparent activities $A_O(E)$ are presented on Fig. 4. An apparent activity, increasing with energy, indicates penetration of gamma-rays through the outer layer. On the other hand, an apparent activity, decreasing with energy, indicates contamination of the inner layer or an effective shield thickness smaller than the nominal thickness, indicating presence of ducts. An activity, independent on energy, indicates the contamination at the outer surface of the inner layer.

The effective thickness of the shield of the spectrometer RA can be assessed from the increase of the apparent activity over its value, A_D. The assessment is done relative to the apparent activity at the lowest energy, where a substantial increase over A_D is observed, i.e. at 609 keV:

$$d(E) = \frac{\ln \frac{A(E) - A_D}{A(609\text{ keV}) - A_D}}{[\mu(609\text{ keV}) - \mu(E)]\rho} \quad .$$

The effective thickness, calculated as a function of energy is presented in Table 2. A slight increase in the average value indicates additional attenuation outside the shield, i.e. in the material, where the gamma-rays are emitted.

The energy dependence of $A_O(E)$ indicates presence of ducts in the spectrometers PB, MO and PO. The effective shield's thickness of these spectrometers can be assessed analogously to the spectrometer RA and amount (1.9 ± 0.2) cm, (5.3 ±0.3) cm and (3.9 ± 0.4) cm respectively. The small effective thickness for the spectrometer PB points to an important duct, what can be observed already in the Fig. 3. Here an increase of the apparent activity at the energy of 352 keV is visible. The spectrometers FE, MG and HG do not have ducts, whereas the increasing energy dependence in the spectrometers SE and BL at the boundary between the inner and outer layer indicate the necessity of of the additional outer layer of the shield. The detector HG exhibits only slight contamination of the detector and/or contamination of the graded layers preventing registration of fluorescence from the shield.

The time dependence of the radon-induced background originates in the variable concentration of radon in the ambient air, which affects the contamination of air within the cavity by the draught through the spectrometer. Variations due to draught were observed on the detectors PO, MG, BL and RA. The critical outdoor temperatures, where the background starts to rise are 15 °C, 14 °C, 20 °C and 18 °C respectively. The largest effect relative to the background below the critical temperature is observed at the energy of 295 keV. The increase of the background at outdoor temperatures exceeding the critical level we describe empirically with a linear function with a slope extracted from the background measurements. In table 3 the slopes for different detectors and different energies are given at energies where calculated slopes differ significantly from zero. It can be observed that the strongest temperature dependence exhibits the spectrometer with the largest cavity with a shield of lead bricks having rifts between bricks. The second largest dependence occurs in the spectrometer where no flushing is performed. These two spectrometers exhibit also the lowest critical temperature. In the spectrometer MG an increase of the slope with energy is observed. This is due to the diffusion of radon into the paraffin layer and the stronger attenuation of gamma-rays in the paraffin at lower energies.

It should be noted that the increase of the background relative to that below the critical temperature may easily reach 100%. Therefore it is of vital importance to take it into account, especially when measuring concentrations of ^{238}U and ^{226}Ra in low-activity samples such as dry residue, obtained after evaporation of water, aerosol filters and water filters of suspended particulates, as described by Korun and Kovačič, 2010.

In routine measurements the time-dependence of the background is taken into account via the measurement of the outdoor temperature. Daily averages of the outdoor temperature are recorded and the background count rates during the measurement time are calculated. These count rates are used for correction of peak count rates in the peaks in the spectra. Here the possible lag of the count rates behind the outdoor temperature is neglected.

Conclusion

For nine spectrometers mounted in the counting room of the Laboratory for Radiological Measuring Systems and Radioactivity Measurements the sources of radon-induced background have been determined. The contributions due to the contamination of the detector, the time-dependent air contamination in the shield cavity and the radiation penetrating the shields were calculated. These data are used for calculation of the radon background during the sample measurement and the calculation of background count rates in peaks, which are to weak to be analyzed reliably. Therefore by the analysis presented the results of routine measurements were improved, especially in measurements of low-activity samples.

References

Korun, M., Kovačič, K., 2010. *^{238}U determination in ground water samples by gamma-ray spectrometry*, submitted for publication to Appl. Radiat. Isot.

Table 1 Characteristics of the detector shields

Spectrometer code	Inner layer		Outer layer		Volume of the shield cavity L
	Material	Thickness cm	Material	Thickness	
FE	iron	15			32
PB	lead	16			5
MO	Lead	12			5
PO	Lead	10			2
MG	Paraffin	10	Lead	12	34
SE	Mercury	1	Lead	10	17
HG	Mercury	1	Lead	12	11
BL	Mercury	1	Lead	10	14
RA	Lead	3 - 5			16

Table 2. The effective thickness of the shield for the spectrometer RA calculated at energies exceeding 609 keV

Energy [keV]	Effective thickness [cm]
768	4.0 ± 0.9
1120	3.8 ± 0.5
1238	3.9 ± 0.5
1764	4.3 ± 0.6
2204	4.6 ±0.6
2247	4.7 ± 0.7

Table 3. The coefficients of the temperature dependence of the background count rate

	Temperature dependence of the count rate / s^{-1}°C^{-1}			
Detector	PO	MG	BL	RA
Critical temperature °C	15	14	20	18
Energy keV				
75		0.015 ± 0.003		
77	0.010 ± 0.003	0.017 ± 0.003	0.013 ± 0.014	
87	0.005 ± 0.002	0.010 ± 0.003		
295	0.011 ± 0.02	0.039 ± 0.004	0.029 ± 0.015	0.0020 ± 0.0006
352	0.010 ± 0.002	0.038 ± 0.004	0.031 ± 0.019	0.0019 ± 0.0006
609	0.011 ± 0.002	0.042 ± 0.005	0.020 ±0.006	0.0019 ± 0.0007
768		0.042 ± 0.005		
1120	0.010±0.003	0.045 ± 0.004	0.036 ± 0.025	0.0007 ±0.0004
1238	0.015 ± 0.008	0.050 ± 0.005		
1764	0.015 ± 0.004	0.055 ± 0.005	0.028 ± 0.023	
2204		0.060 ± 0.007		

Figure captions

Fig. 1 Seasonal variations of the count rate of the peak at 352 keV in background measurements on the spectrometer MG

Fig. 2. The temperature dependence of the count rate in the peak at 352 keV in the background measurements on the spectrometer MG

Fig. 3. The energy dependence of the apparent activities for nine spectrometers

Fig. 4. The energy dependence of the apparent activities $A_{\mathrm{O}}(E)$

Figure 1

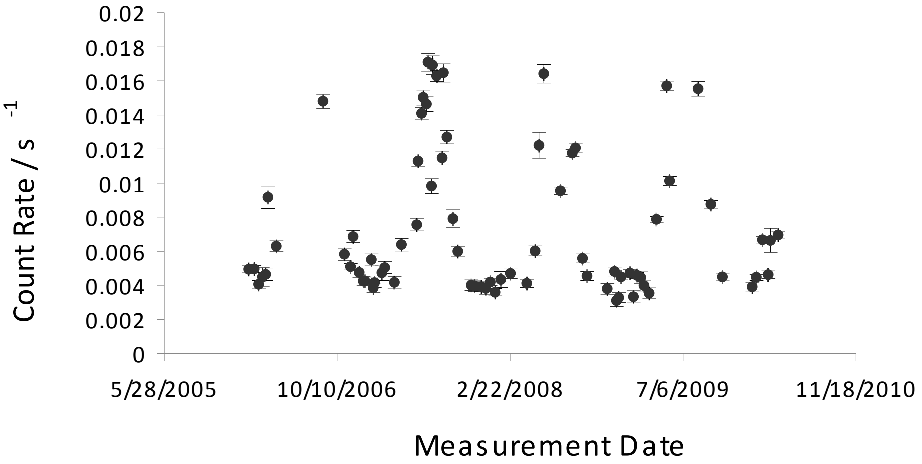
Count Rate / s $^{-1}$
0.02
0.018
0.016
0.014
0.012
0.01
0.008
0.006
0.004
0.002
0
5/28/2005
10/10/2006
2/22/2008
7/6/2009
11/18/2010
Measurement Date

Figure 2.

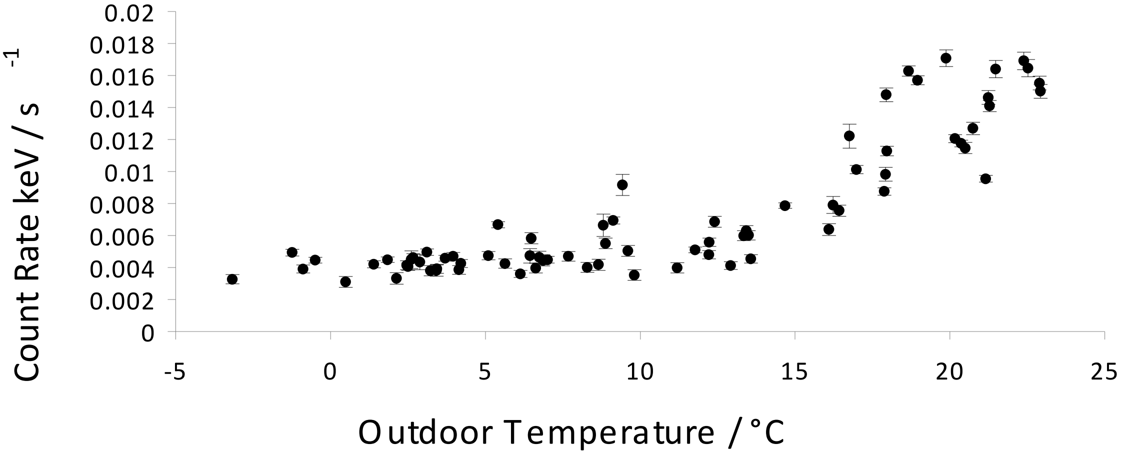
0.02
0.018
0.016
0.014
0.012
0.01
0.008
0.006
0.004
0.002
0
Count Rate keV / s -1
-5
0
5
10
15
20
25
Outdoor Temperature / °C

Figure 3

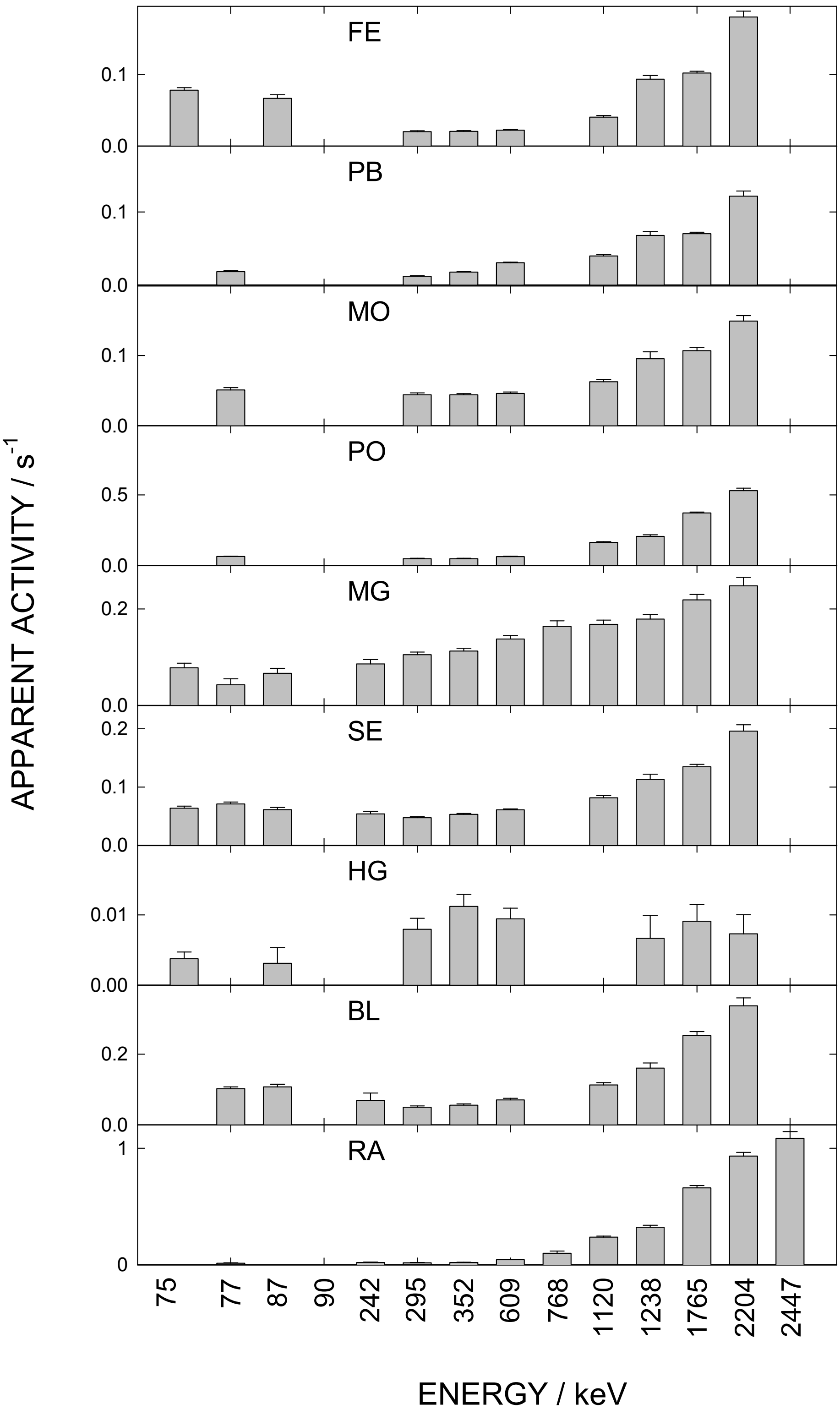
FE
PB
MO
PO
MG
SE
HG
BL
RA
0.0
0.1
0.5
0.2
0.00
0.01
0
1
APPARENT ACTIVITY / s^{-1}
75
77
87
90
242
295
352
609
768
1120
1238
1765
2204
2447
ENERGY / keV

Fig. 4

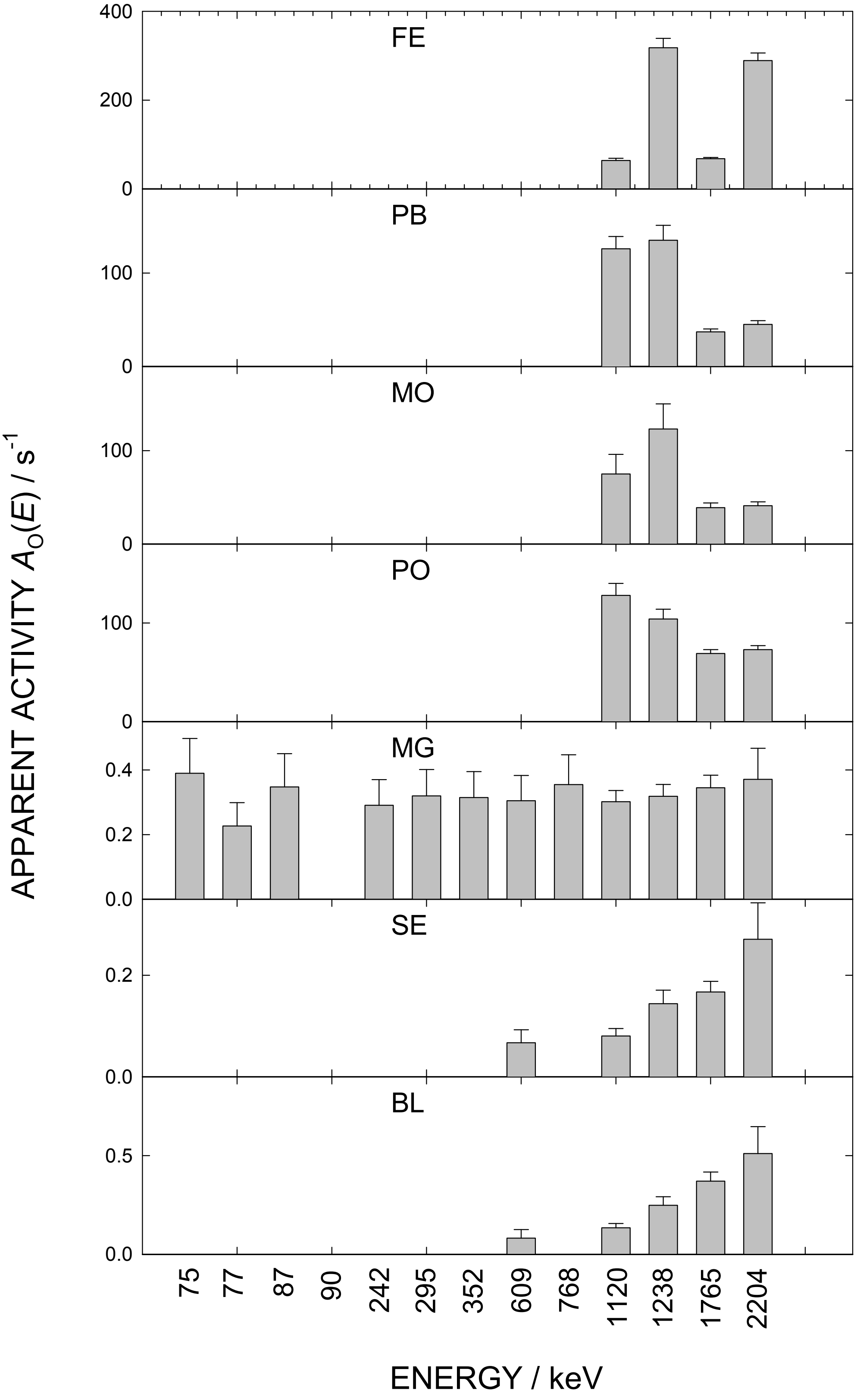
APPARENT ACTIVITY $A_O(E)$ / s^{-1}
FE
400
200
0
PB
100
0
MO
100
0
PO
100
0
MG
0.4
0.2
0.0
SE
0.2
0.0
BL
0.5
0.0
75
77
87
90
242
295
352
609
768
1120
1238
1765
2204
ENERGY / keV

Elsevier Editorial System(tm) for Applied Radiation and Isotopes
Manuscript Draft

Manuscript Number: ARI-D-11-00035

Title: A comparative study of radon-induced background in low-level gamma-ray spectrometers

Article Type: Full Length Article

Section/Category: Radioactivity and Radiation Measurements

Keywords: Gamma-ray spectrometers, Radon-induced background, Attenuation coefficients, 226Ra

Corresponding Author: Dr. Matjaz Korun,

Corresponding Author's Institution:

First Author: Petra Maver Modec

Order of Authors: Petra Maver Modec; Matjaz Korun; Matej Martelanc; Branko Vodenk

Manuscript Region of Origin: SLOVENIA

Abstract: The radon-induced background of ten high-resolution germanium gamma-ray spectrometers was analyzed. In the analysis the apparent activity was introduced, which is defined as the peak count rate normalized with respect to emission probability and detection probability. On the basis of its energy and time dependence the contributions to the background count rates due to the radiation, penetrating the shield, and the radiation due to the contamination of the air with radon daughters, were determined.

A comparative study of the radon-induced background in low-level gamma-ray spectrometers

P. Maver Modec[1,2], M. Korun[*1], M. Martelanc[3], B. Vodenik[1]

[1]"Jožef Stefan Institute", Jamova cesta 39, Ljubljana, Slovenia
[2]Jožef Stefan International Postgraduate School, Jamova cesta 39, Ljubljana, Slovenia
[3]Faculty of Computer and Information Science, Tržaška cesta 25, Ljubljana, Slovenia

Abstract: The radon-induced background of ten, high-resolution, germanium, gamma-ray spectrometers was analyzed. In the analysis the apparent activity was introduced, which is defined as the peak count rate normalized with respect to the emission probability and the detection probability. On the basis of its energy and time dependence, the contributions to the background count rates due to the radiation penetrating the shield and the radiation due to the contamination of the air with radon daughters were determined.

Keywords: Gamma-ray spectrometers, Radon-induced background, Attenuation coefficients, ^{226}Ra

Introduction

Gamma-ray spectrometry is a method that is not very sensitive when applied to activity measurements of ^{226}Ra. This isotope radiates gamma-rays mainly at 186 keV, with a probability of about 3.5% (IAEA 2007). Unfortunately, these gamma-rays interfere with the gamma-rays from the decay of ^{235}U, which introduces an additional source of uncertainty to the measurement results of

---

[*] Corresponding author. Tel.:+386 1 4773 900; fax: +386 1 4773 151; E-mail address: matjaz.korun@ijs.si (M. Korun).

samples containing uranium (Ebaid, 2009). For this reason, it might, therefore, be advantageous to determine the radium activity from the activity of the radon daughters ^{214}Pb and ^{214}Bi, which radiate at many gamma-ray energies in the energy range from 200 keV to 2500 keV and at bismuth X-ray energies. The emission probabilities for these photons can reach up to 45%. Consequently, this indirect measurement method is more sensitive than a direct determination based on the 186-keV gamma-ray peak.

If the activity of the ^{226}Ra in the sample is small, a substantial part of the count rate of the peaks, signaling the presence of radon daughters, may originate from the spectrometer background. In the spectral analysis this systematic influence is accounted for by the subtraction of the background, i.e., the peak count rates measured in the absence of the sample. Therefore, it is of vital importance to accurately determine the radon-induced spectrometer background.

The influence of radon daughters on the spectrometer background originates from the presence of the ^{226}Ra in the detector, the shielding materials, the materials surrounding the spectrometer shield, where the rays penetrating the shield originate, and from the presence of radon daughters in the air that fills the shield's cavity. While the contributions from the contamination of the detector, the shielding materials and the environment are constant with time, the contribution due to the contamination of the air may vary. The concentration of radon daughters in the air in the cavity follows their concentration in the air in the counting room, which is not constant (WHO 2009). Therefore, the count rate in the peaks in the background due to radon daughters may vary with time and cannot be determined as a simple average over the count rates obtained from repeated background measurements. The radon-induced background also increases the continuous spectral background, thereby affecting the measurement sensitivity for other gamma-ray emitters.

It is the purpose of this contribution to present an analysis of the radon-induced background of the spectrometers installed in the Laboratory for Radiological Measuring Systems and Radioactivity Measurements in order to determine the sources of contamination, their location, their contribution to the background and its time dependence.

Materials and Methods

The counting room is located in a basement, below ground level. It is kept at a constant temperature and is not ventilated so as to avoid any possible contamination (the air is exchanged only as a result of the draught). This draught is stronger when there are low outdoor temperatures, since then the cooler air from the ambient of the building tends to replace the warmer air in the counting room. There is a large amount of radon entering the counting room because of the poor hydroisolation of the building. Radon can enter the room by advection through the gap between the foundation wall and the concrete floor slab, and by diffusion through the walls (UNSCEAR 2000). This advection is constant throughout the year since the temperature of the air in the counting room and the temperature of the soil are constant. However, the diffusion through the walls is greater in summer, since during this time the atmospheric air cannot replace the subterranean air and dilute the radon that is there (Sundal et al, 2008). During the summer the radon concentration in the counting room may reach 600 Bq/m^3, but in the winter the average concentration is 70 Bq/m^3. Diurnal variations of the radon concentration are not taken into account since the typical counting time for routine measurements lasts at least one day.

The counting room houses ten spectrometers with high-resolution, germanium spectrometers that have a variety of different characteristics. The characteristics of the spectrometer shields are given in Table 1. However, the graded layers used to prevent the registration of the X-rays are omitted from the table in order to improve its clarity. The shield cavities, except for the cavities of the spectrometers PO and LE, are flushed constantly with nitrogen in order to remove the ambient air, which is contaminated with radon, from the interior of the shield. The nitrogen is obtained by evaporating liquid nitrogen, which is then aged for two weeks to allow the radon to decay. The average daily evaporation rate of the liquid nitrogen is ten liters. Because of the limited supply of nitrogen, some shields are not flushed completely; therefore, some contamination of the radon daughters may remain within the cavity. This is reflected in the seasonal variations of the background of the radon daughters in some spectrometers, which occurs in spite of the flushing. The seasonal variations of the count rate for the peak at 352 keV in the background measurements of the spectrometer MG, which has the largest shield cavity, are presented in Fig. 1. In Fig. 2 this peak count rate is presented as a function of the outdoor temperature, averaged over the counting time of the measurement. The total count rate in the spectral energy interval from 45 keV to 2700 keV is larger by about 20% in the summer than in the winter for this detector.

The background measurements are performed at times when samples for the activity measurements are not available. The acquisition time for the background measurements is between 3 days and 12 days. Like with other peaks occurring in the background spectrum, the count rate in the peaks of the radon daughters is determined from the measured spectra under the same peak-analyzing conditions as the sample spectra. Some of the peaks are not identified in all the background measurements because of the poor statistics or the poor deconvolution of the multiplets when the statistical uncertainties of the peak areas are high. Here we analyze only the count rates at energies where the peaks are recognized in a great majority of the measurements. These peaks occur at energies of 75 keV, 77 keV, 87 keV, 90 keV, 242 keV, 295 keV, 352 keV, 609 keV, 768 keV, 1120 keV, 1238 keV, 1765 keV, 2204 keV and 2448 keV. Some of these energies are omitted from the data on the spectrometers where the peaks are not recognized in the background measurements frequently enough. Also, the X-ray energies are omitted for the spectrometers where radon-daughter-induced peaks interfere with the peaks due to the fluorescence of the lead that constitutes the spectrometer shields and the uranium from the detector materials.

Results

It is clear from Fig. 1 that the count rates in the background peaks may be subject to seasonal variations. However, below a critical outdoor temperature the count rate no longer depends on it, since at this point the radon concentration is low enough for the flushing to effectively remove all of the radon from the shield cavity. The effectiveness of the flushing depends on the volume of air in the cavity, the intensity of the flushing and the permeability of the shield with respect to the air. For the detectors that exhibit a temperature dependence, this critical temperature varies between 14 °C and 20 °C. The count rate below the critical temperature is determined, in addition to the detector efficiency, by the contamination of the detector and the shield with ^{226}Ra and by the penetration rate of the gamma-rays from the counting room through the shield. Above the critical temperature the count rate increases linearly with the outdoor temperature. The rate at which it increases depends on the effectiveness of the flushing, the volume of the shield cavity and the efficiency of the detector.

During the background measurements the detector measures the flux of gamma-rays at the center of the shield's cavity, where it is placed. To convert the count rates into gamma-ray fluxes, characterizing the contaminations, the response of the detector and the probability of the emission of the gamma-rays has to be taken into account. To assess the fluxes, the apparent activities $A(E)$ are calculated as

$$A(E) = \frac{n(E)}{\eta(E)b(E)} \qquad ,$$

where $n(E)$ denotes the count rate in the peak at the energy E; $\eta(E)$ is the counting efficiency of a point source, positioned at the detector surface on the symmetry axis of the detector cap, radiating gamma-rays with the energy E; and $b(E)$ is the probability for the emission of gamma-rays with the energy E in a decay of a radon daughter. It is advantageous to use apparent activities for analyzing the background since they are smooth functions of the gamma-ray energy. It follows that the value of an apparent activity does not represent the result of an assessment of a true activity, but serves only for treating the count rates in peaks at different energies on an equal footing. It is possible to interpolate the apparent activities to energies, where the background peaks' count rates are too weak to be measured reliably. Also, from their energy dependence it is possible to deduce simplified models of shields for describing the transport of gamma-rays and compare the apparent activities in different spectrometers.

It should be noted that the point-source efficiency, which is used for the calculation of the apparent activities, only poorly represents the average probability for the registration of a gamma-ray impinging at a large angle on the detector cap. The point-source efficiency used corresponds to a geometry where the rays impinge on the crystal under all angles, describing the probability for the registration of a photon emitted isotropically from a point source. Although the point-source efficiency used is a maximum, it still underestimates the average probability, except in the case of the contamination of the detector cap. Therefore, the apparent activities overestimate the flux rates, normalized to an emission probability of unity. Fig. 3 presents the apparent activities, corresponding to count rates in the spectrum below the critical outdoor temperature, for the spectrometers installed in the counting room.

Above the critical temperature, the background count rate is the sum of the count rate below the critical outdoor temperature and the contribution due to the variable concentration in the ambient air, which affects the contamination of the air within the shield cavity of the draught through the spectrometer shield. The count rate is described as:

$$n'(E,T) = n(E) + k(E)(T - T_c) \qquad ,$$

where T denotes the average outdoor temperature during the background measurement, T_c is the critical outdoor temperature and $k(E)$ is the rate of increase of the background count rate in the peak at an energy E with temperature. Like with the apparent activity, the apparent activity due to the air contamination, normalized to the unit of the temperature increase above the critical temperature, can be calculated as

$$A_T(E) = \frac{n'(E,T) - n(E)}{\eta(E)b(E)(T - T_c)} = \frac{k(E)}{\eta(E)b(E)} \qquad .$$

For the detectors exhibiting a temperature dependence the increase in the apparent activity with temperature is presented in Fig. 4 at energies where the peaks in the background spectra are strong enough to allow its evaluation. For other detectors it can be assumed that the critical temperature exceeds the maximal average outdoor temperature where the background measurements were performed. The importance of the temperature dependence relative to the temperature-independent background is presented in Table 2, together with the critical temperature T_c. The relative influence is calculated as the ratio of the rate of increase of the apparent activity with temperature $A_T(E)$ versus the temperature-independent apparent activity, averaged over the energies in the energy interval from 200 keV to 400 keV, where the apparent activity is at a minimum, and multiplied by the temperature difference between 25^{o}C, which is the maximal average outdoor temperature, and the critical outdoor temperature T_c. This ratio gives the maximal relative influence of radon daughters in the air of the counting room on the radon-induced spectrometer background.

Discussion

It is clear from Fig. 3 that in the energy range above 500 keV the temperature-independent apparent activity increases with the energy in all the spectrometers, except LE and HG. The spectrometer LE has a low-energy detector, having a crystal with a thickness of only 1 cm having small peak efficiency at energies exceeding 500 keV. On the other hand, the detector HG has a very low background and the incidence of the detection of the radon-induced background peaks above an energy of 500 keV does not exceed 30%. In these circumstances the reliability of the peak analysis is not sufficient to yield trustworthy results. In other detectors, the apparent activity is an increasing function of the energy. This is due to the attenuation coefficient for the photons in the shielding material, which decreases with energy. The rate of increase carries information about the thickness of the material between the source of the photons and the detector. In the absence of ducts in the shielding, below 500 keV the photons cannot penetrate the layers of the shielding; therefore, here the apparent activity, A_D, is given by the contamination of the detector and the inner surface of the cavity with the ^{226}Ra. The increase of the apparent activities over this level indicates there are contributions from the shielding material and from the exterior of the shield.

The count rate in the X-ray peaks is difficult to interpret in terms of contamination because of the X-ray fluorescence of lead, which interferes with the X-ray peaks from the ^{214}Bi that belong to the decay of the radon daughters. Namely, the graded layers (made of cadmium and copper) do not attenuate the fluorescence completely. They also interfere with gamma-rays from the decay of the ^{235}U at energies of 75 keV and 90 keV. In addition, the deconvolution of the multiplets is not reliable for the large statistical uncertainties of the peak areas. Therefore, the apparent activities at the energies that coincide with the energy of the lead X-rays (75 keV and 87 keV) are only given in cases where no lead is used in the shielding or where the inner layer absorbs the fluorescent X-rays completely and where the decomposition of the multiplets is reliable enough. They are also not given when gamma-rays from the uranium decay are present in the background spectrum. It is clear from Fig. 3 that the apparent activities calculated from the X-ray peak roughly reproduce the apparent activities due to the detector contamination, except on the spectrometer FE, where the increased apparent activity indicates the presence of lead within the detector.

A rough estimate of the quality of the spectrometer shields, where an increase of the apparent activity at energies above 500 keV is observed, can be obtained from the ratio of the apparent activities at 1765 keV and 352 keV. The values of this ratio are presented in Table 3. The maximal value is attained for the spectrometer RA, which has an improvised lead shield and consequently a large penetration for high-energy gamma-rays. The next-highest values are associated with the spectrometers PO and BL, with portable detectors. Only the detector cap of these detectors is shielded, and therefore the gamma-rays impinging through the detector dewar are considerably less attenuated. The spectrometer SE has a portable detector as well, but its dewar is contained within the shielding together with the detector cap. The other spectrometers FE, PB, MO and MG have detectors with a vertical dipstick. The dipstick of the detector MG has an internal shielding that prevents the photons flying near the cold finger to impinge on the detector crystal. The spectrometer FE has an iron shield, which is reflected in a relatively high value of the ratio.

If the spectrometer shield consists of only one layer, its effective thickness can be assessed from the increase in the apparent activity over its minimal value, A_D. The flux inside the cavity can be expressed as

$$A(E) - A_D = A_o e^{-\mu_S(E)\rho_S d} \quad ,$$

where $\mu_S(E)$, ρ_S and d denote the attenuation coefficient for the gamma-rays in the shield, the shield density and its thickness, respectively. A_0 denotes the apparent activity in the absence of the shielding. At high energies this apparent activity depends only weakly on the energy, since here the attenuation coefficient in the building materials, from which the gamma-rays are emitted, weakly depends on the energy. For the purpose of assessing the effective thickness of the shielding with an atomic number much higher than the average atomic number of the building materials it can be assumed to be independent of the energy. Then the assessment can be made on the basis of the increase of the apparent activity over A_D at the lowest energy, where this increase is substantially larger than its uncertainty. For the detectors PB and RA, at 609 keV such an increase already occurs. Here, the effective thickness can be estimated from

$$d(E) = \frac{\ln \dfrac{A(E) - A_D}{A(609\ \mathrm{keV}) - A_D}}{[\mu_S(609\ \mathrm{keV}) - \mu_S(E)]\rho_S} \qquad .$$

The effective thickness, calculated as a function of the energy, is presented in Table 4. In the detector RA a slight increase in the average thickness with energy indicates an additional attenuation outside the shield, i.e., in the material, where the gamma-rays are emitted. The relatively low average thickness for the detector PB points to a narrow duct where the detector is shielded with only approximately 1 cm of lead. For the detectors FE, MO and PO the effective thickness is assessed relative to the apparent activity at 1120 keV to 16 cm ± 2 cm, 9 cm ± 2 cm and 6 cm ± 1 cm, respectively. The values for the effective thickness reproduce well the average thickness of the shield, taking into account the variability of the shield thickness with respect to the direction of the impinging gamma-rays.

For the spectrometers with a shield consisting of two layers, the flux of gamma-rays at the outer surface of the inner layer, $A_\mathrm{O}(E)$, can be calculated from the increase of the apparent activity over its value A_D, corrected for the attenuation of the gamma-rays in the inner layer. This is calculated as

$$A_O(E) = (A(E) - A_D)e^{\mu_I(E)d_I\rho_I} \qquad ,$$

where $\mu_\mathrm{I}(E)$, d_I and ρ_I denote the attenuation coefficient, the thickness and the density of the material of the inner layer, respectively. This calculation can be performed for the spectrometers MG, SE and BL, having two-layered shields and exhibiting an increase in the apparent activity with energy. For the detector MG, which does not exhibit a constant apparent activity in the region 200–400 keV, a value of zero has been assumed for A_D. The apparent activities $A_\mathrm{O}(E)$ are presented in Fig. 5. It is clear from the figure that the apparent activity is independent of the energy for the detector MG. It follows that the contamination is located at the outer surface of the paraffin. Here, no evidence of the penetration of gamma-rays through the outer layer exists. On the other hand, the increase of the apparent activity for the detectors SE and BL indicates the penetration of the gamma-rays through the outer layer. The penetration is stronger in the spectrometer BL, since here the ratio A_O(1120 keV)/A_O(609 keV) is larger, which indicates a smaller effective thickness. The difference reflects the effectiveness of the shielding of the portable dewar of the spectrometer SE.

The time dependence of the radon-induced background originates from the variable concentration of the radon in the air in the counting room, which affects the contamination of the air within the spectrometer cavity as a result of the draught through the shielding. The variations due to the draught were observed on the spectrometers LE, PO, MG, BL and RA. For these detectors the critical outdoor temperatures, where the background starts to increase, are 17 $^{\mathrm{o}}$C, 15 °C, 14 °C, 20 °C and 18 °C, respectively. The largest effect of the temperature dependence relative to the background below the critical temperature is observed at an energy of 295 keV. It is clear from Fig. 4 that the rate of the increase is, in the framework of the accuracy achieved, independent of the energy for the spectrometers LE, PO and BL. For spectrometers showing an energy-independent rate of increase A_{T} it can be concluded that the contamination causing the temperature dependence is located within the shield cavity. Fig. 6 presents the rate of increase of the apparent activity $A'_{\mathrm{T}}(E)$ for the spectrometer MG, corrected for the attenuation in the paraffin layer, calculated as

$$A'_T(E) = A_T(E)e^{\mu_P(E)\rho_P d_P} \quad ,$$

where $\mu_{\mathrm{P}}(E)$, ρ_{P} and d_{P} denote the attenuation coefficient of the gamma-rays, the density and the thickness of the paraffin layer. Since the corrected rate does not depend on the energy it follows that the corresponding contamination is located on the outer side of the paraffin layer. This deduction supports the conclusion regarding the location of the apparent activity on the detector MG.

The rate of increase of the apparent activity with temperature, which is independent of the energy for all the spectrometers, except for the spectrometer RA, offers the opportunity to treat the temperature dependence of the radon-induced background at all energies on an equal footing. The spectrometer RA exhibits an energy dependence, since here the temperature dependence originates, at least partially, in the increased radon concentration in the air of the counting room, i.e., outside the lead shielding. It is obvious that here the high-energy gamma-rays penetrate through the shield with a probability that is high enough to detect variations in the concentrations of the radon daughters in the ambient air, although the variability of the background with the temperature is small compared to the background independent of the temperature.

To describe the temperature dependence better, for the spectrometers LE, PO, MG and BL the average rates of increase were calculated. These averages are presented in Table 5. The largest average is exhibited by the spectrometer MG. Here the radon diffuses into the paraffin, causing its contamination with radon daughters. Although flushing the cavity prevents radon from entering the cavity, it does not prevent it from contaminating the paraffin. The cavities of the spectrometers LE and PO are not flushed, which results in a considerable temperature dependence, in spite of their low volumes. The high temperature dependence of the spectrometer BL is due to the relatively poor tightness of its shield and consequently to a large draught through its cavity.

It should be noted that the increase in the background relative to that below the critical temperature can in some spectrometers easily exceed 100%. Therefore, it is of vital importance to take this into account, especially when measuring the concentrations of the ^{238}U and ^{226}Ra in low-activity samples, such as the dry residue obtained after the evaporation of water, aerosol filters and water filters of suspended particulates, as described by Korun and Kovačič (2010).

In routine measurements the time dependence of the background is taken into account via measurements of the outdoor temperature. The daily averages of the outdoor temperature are recorded and the background count rates during the measurement time are calculated. These count rates are used when correcting the peak count rates in the sample spectra.

Conclusion

For the ten spectrometers mounted in the counting room of the Laboratory for Radiological Measuring Systems and Radioactivity Measurements the sources of radon-induced background were determined. The apparent activity, which was introduced to connect the background count rates at different energies, proved to be a useful quantity enabling their systematic analysis. The contributions due to the penetration through the shield and the contamination of the air with radon daughters were determined on the basis of the energy and temperature dependence of the apparent activities. It was shown that in the case when the contamination resides within the shield, the temperature dependence of the apparent activity does not depend on the gamma-ray energy. Therefore, the calculations of the time-dependent background count rates could be improved. Also, the background count rates in the peaks that are too weak to be analyzed reliably were determined. As a consequence, regarding the measurement results of low-activity samples, some systematic influences were removed and the uncertainties reduced.

References:

Ebaid, Y. Y., 2008. Use of gamma-ray spectrometry for uranium isotopic analysis in environmental samples, Rom. Journ. Phys. 55, 69 - 74

IAEA 2007: Update of X-ray and gamma-ray decay data standards for detector calibration and other applications, International Atomic Energy Agency, Vienna

Korun, M., Kovačič, K., Determination of ^{238}U in ground water samples gamma-ray spectrometry. Appl. Rad. Isot. (2010), doi:10.1016/j.apradiso.2010.12.010.

Sundal, A.V., Valen, V., Sodal, O., Strand, T., 2008. The influence of meteorological parameters on soil radon levels in permeable glacial sediments, Sci. Tot. Environ. 389, 418-428.

UNSCEAR, 2000. Sources and effects of ionizing radiation. Report to the General Assembly with Scientific Annexes, YN, New York.

WHO 2009: WHO handbook on indoor radon, WHO press, Geneva, Switzerland.

Table 1. Characteristics of the detector shields

Spectrometer code	Inner layer		Outer layer		Volume of the shield cavity L
	Material	Average thickness cm	Material	Thickness	
FE	Iron	15			32
PB	Lead	16			5
MO	Lead	12			5
LE	Plexy	2	Lead	10	1
PO	Lead	10			2
MG	Paraffin	10	Lead	12	34
SE	Mercury	1	Lead	10	17
HG	Mercury	1	Lead	12	11
BL	Mercury	1	Lead	10	14
RA	Lead	3–5			16

Table 2. The critical outdoor temperature T_c and the influence of the temperature dependence relative to the temperature-independent background for the detectors exhibiting a time variation of the radon-induced background.

Detector code	Critical outdoor temperature [^{o}C]	Relative influence
LE	17	2.2 ± 0.3
PO	15	2.2 ± 0.3
MG	14	3.4 ± 0.3
BL	20	1.2 ± 0.1
RA	18	1.1 ± 0.2

Table 3. The ratio *A*(1765 keV)/*A*(352 keV) for the detectors exhibiting an increase of the apparent activity with energy.

Detector code	*A*(1765 keV)/*A*(352 keV)
FE	4.9 ± 0.2
PB	3.9 ± 0.2
MO	2.3 ± 0.4
PO	7.6 ± 0.3
MG	1.9 ± 0.1
SE	2.5 ± 0.1
BL	6.3 ± 0.8
RA	33.1 ± 3.0

Table 4. The effective thickness of the shield for the spectrometers PB and RA calculated at energies exceeding 609 keV

Energy [keV]	Effective thickness [cm]	
	PB	RA
768		4.1 ± 0.6
1120	0.9 ± 0.1	4.0 ± 0.3
1238	2.1± 0.3	4.0 ± 0.4
1764	1.9 ± 0.1	4.4 ± 0.2
2204	2.6 ± 0.1	4.7 ±0.2
2447		4.8 ± 0.2

Table 5. The average rate of increase with temperature above the critical temperature of the apparent activity for different spectrometers

Detector code	LE	PO	MG	BL
Average rate [10^{-3} s^{-1} $^{o}C^{-1}$]	2.8 ± 0.8	10.9 ± 1.7	103 ± 6	15.4 ± 1.8

Figure captions:

Fig. 1. Seasonal variations of the count rate of the peak at 352 keV in background measurements on the spectrometer MG

Fig. 2. The temperature dependence of the count rate in the peak at 352 keV in the background measurements on the spectrometer MG

Fig. 3. The energy dependence of the apparent activity $A(E)$ for the ten spectrometers

Fig. 4. The rate of increase of the apparent activity $A_{\mathrm{T}}(E)$ at temperatures above the critical temperature

Fig. 5. The energy dependence of the apparent activities $A_{\mathrm{O}}(E)$

Fig. 6. The energy dependence of the rate of increase of the apparent activity for the detector MG, corrected for the attenuation in the paraffin layer, $A'_{\mathrm{T}}(E)$

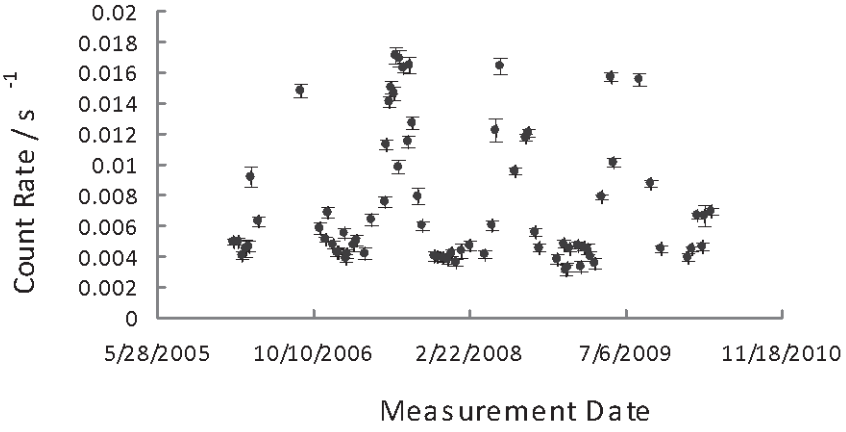
0.02
0.018
0.016
0.014
0.012
0.01
0.008
0.006
0.004
0.002
0
Count Rate / s^{-1}
5/28/2005
10/10/2006
2/22/2008
7/6/2009
11/18/2010
Measurement Date

Figure(s)

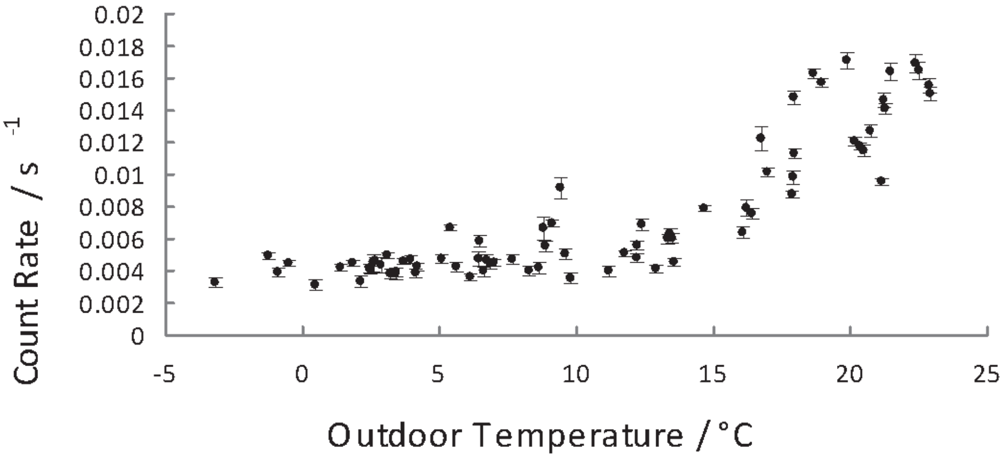

Count Rate / s^{-1}
0.02
0.018
0.016
0.014
0.012
0.01
0.008
0.006
0.004
0.002
0
-5
0
5
10
15
20
25
Outdoor Temperature / °C

Figure(s)

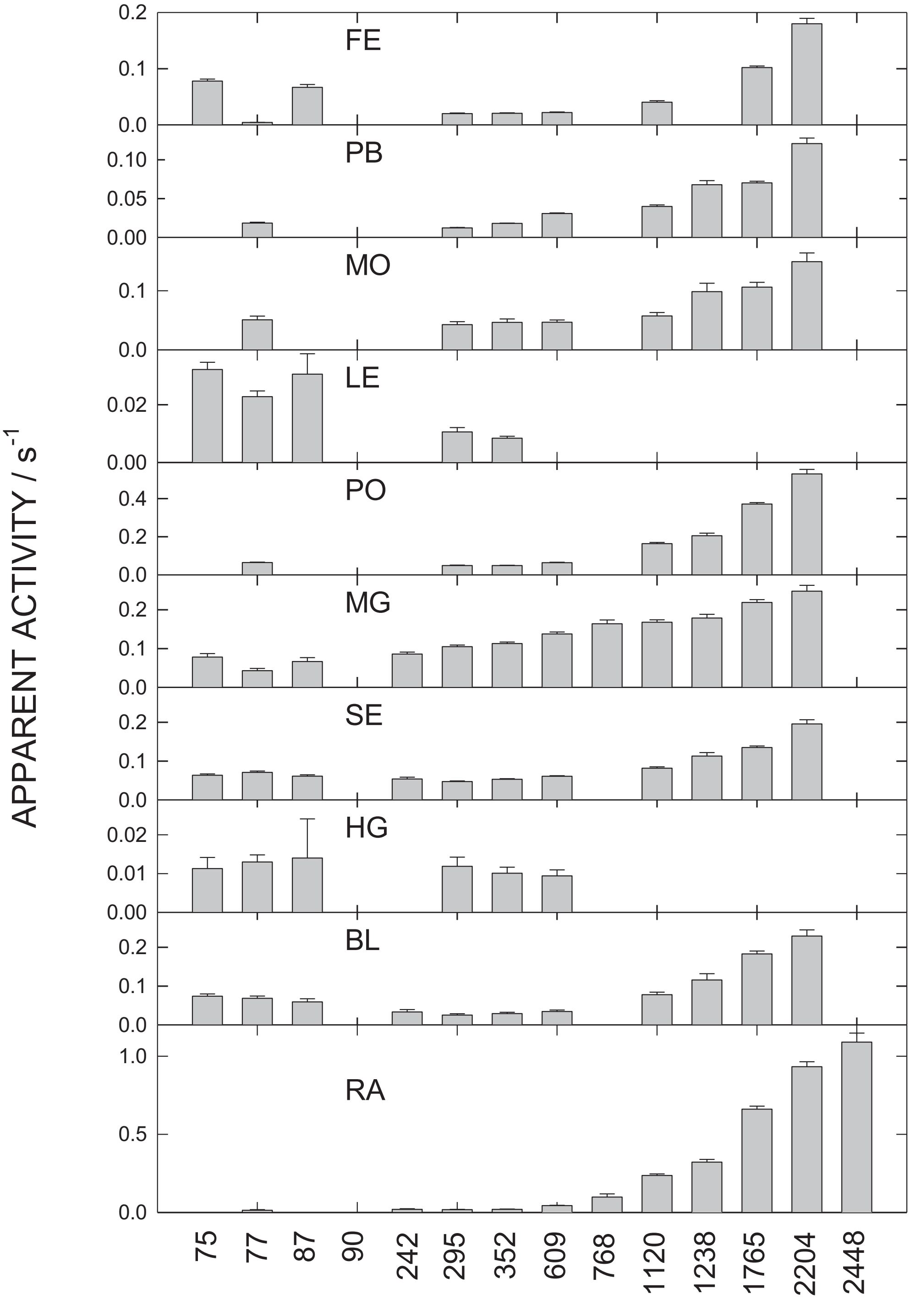
FE
PB
MO
LE
PO
MG
SE
HG
BL
RA
0.2
0.1
0.0
0.10
0.05
0.00
0.1
0.0
0.02
0.00
0.4
0.2
0.0
0.2
0.1
0.0
0.2
0.1
0.0
0.02
0.01
0.00
0.2
0.1
0.0
1.0
0.5
0.0
APPARENT ACTIVITY / s^{-1}
75
77
87
90
242
295
352
609
768
1120
1238
1765
2204
2448
ENERGY / keV

Figure(s)

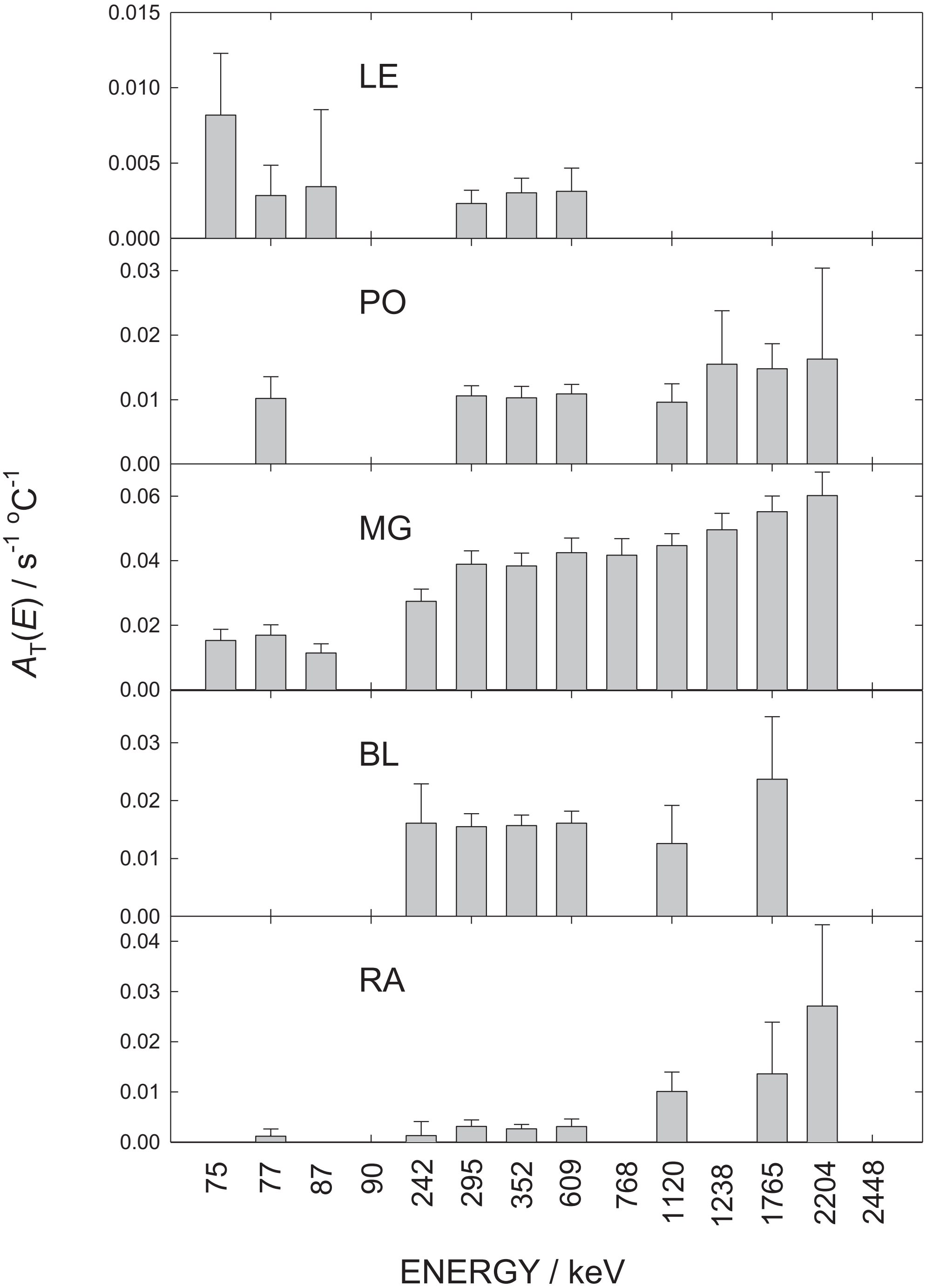
LE
PO
MG
BL
RA
0.015
0.010
0.005
0.000
0.03
0.02
0.01
0.00
0.06
0.04
0.02
0.00
0.03
0.02
0.01
0.00
0.04
0.03
0.02
0.01
0.00
$A_T(E)$ / s^{-1} $^oC^{-1}$
75
77
87
90
242
295
352
609
768
1120
1238
1765
2204
2448
ENERGY / keV

Figure(s)

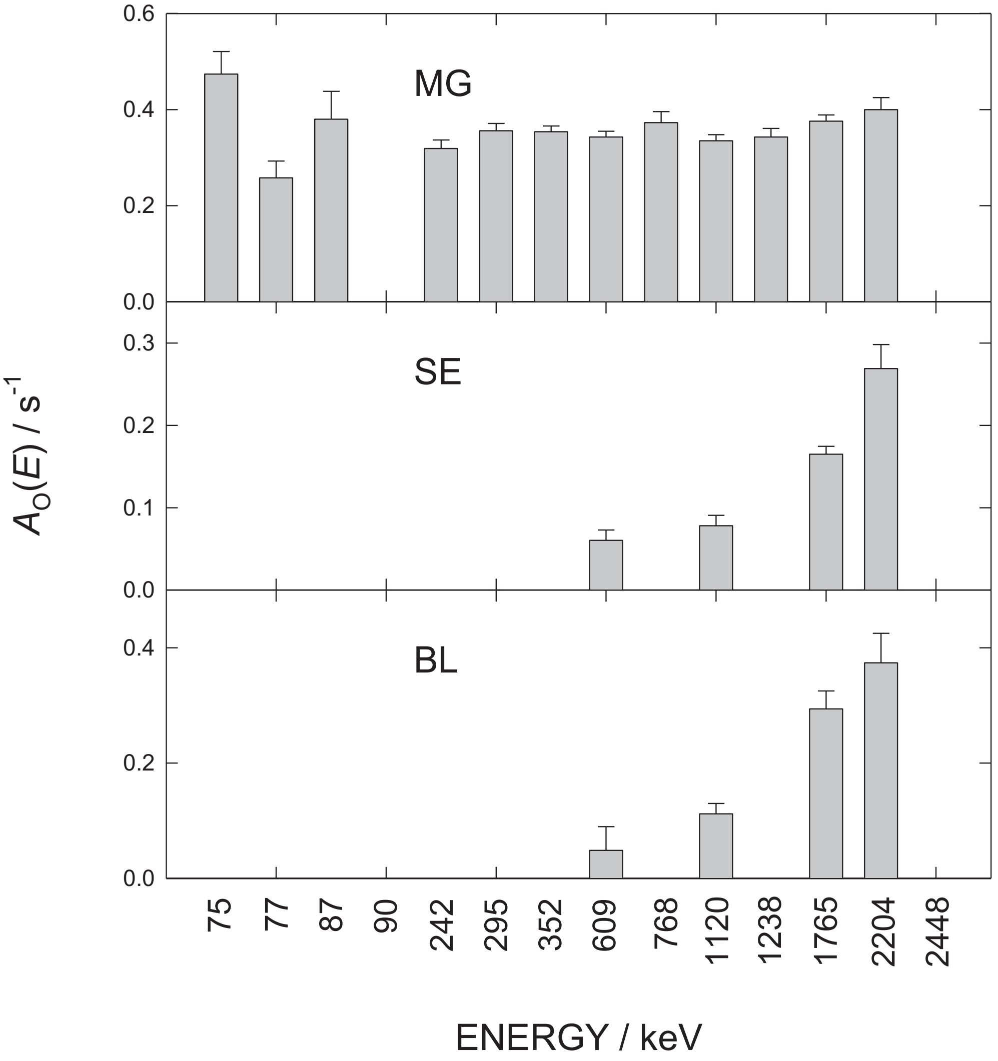

0.6
0.4
0.2
0.0
MG
0.3
0.2
0.1
0.0
SE
0.4
0.2
0.0
BL
$A_O(E)$ / s^{-1}
75
77
87
90
242
295
352
609
768
1120
1238
1765
2204
2448
ENERGY / keV

Figure(s)

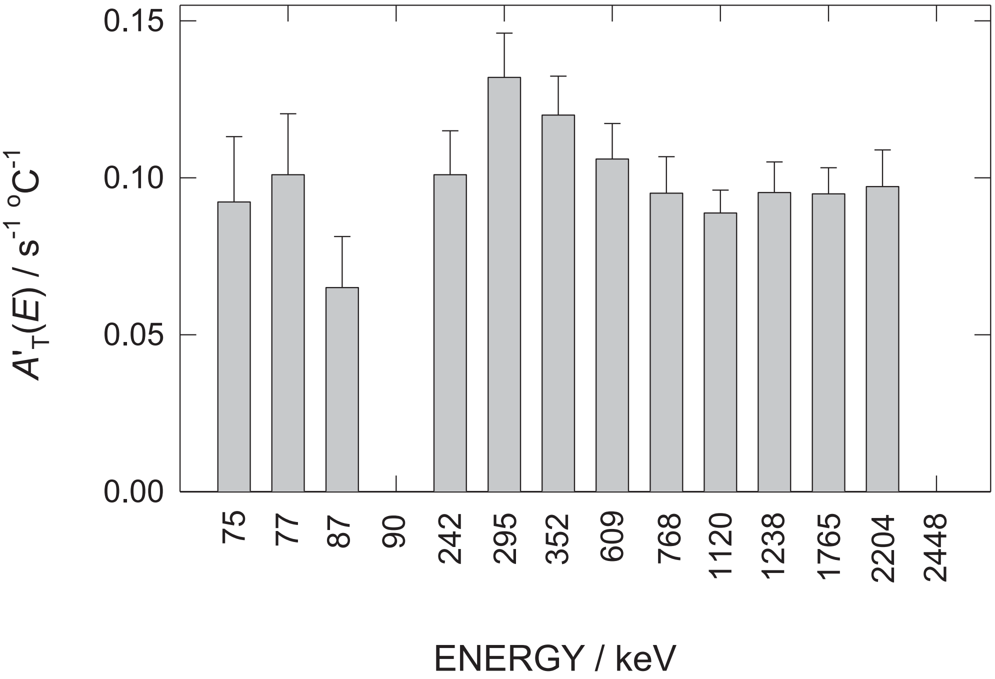

0.15
0.10
0.05
0.00
$A'_T(E)$ / s^{-1} °C^{-1}
75
77
87
90
242
295
352
609
768
1120
1238
1765
2204
2448
ENERGY / keV

TRITIUM AND GAMMA-RAY EMITTERS IN SLOVENIAN GROUNDWATERS

Katarina Kovačič • Jasmina Kožar Logar • Matjaž Aleš Korun

Department of Low and Medium Energy Physics, Institute Jožef Stefan, Jamova cesta 39, SI-1000 Ljubljana, Slovenia.

ABSTRACT. Concentrations of tritium, gamma-ray emitters in the uranium and thorium decay chains (U-238, Th-234, Pb-210, Ra-228, Ra-226 and Th-228) and potassium were measured in samples of ground water in Slovenia. Correlations among Ra-226, Ra-228 and Th-228 were observed in samples from intergranular and fractured aquifers. It was also found that the variability of tritium activity in intergranular aquifers is the largerest and in fractured ones the smallest.

INTRODUCTION

Slovenia gets a large proportion of drinking water from shallow alluvial, fractured and karstic aquifers which supply more than 97% of Slovenian population. In order to manage these groundwaters properly it is advantageous to know their properties and also their vulnerability.

The Directive 2000/60/EC of the European Parliament and of the Council of 23 October 2000 sets out general provisions for the protection and conservation of groundwater for all Member States. To provide better regulation and control on groundwater environmental state the Ministry of the Environment and Spatial Planning of Slovenia established Rules determining the groundwater water bodies. According to the rules 21 water bodies were determined on the basis of existing hydrological, geological, pedological data, data on land use and anthropogenic load (OJ RS 2005).

In 2008 a research project started with cooperation of the Jožef Stefan Institute, the Geological Survey of Slovenia and Ljubljana waterworks. The aim of the project is to find a suitable methodology that could provide us with the information about the age of the groundwater and the correlations between the dynamics, lithology and hydrogeological properties of the aquifers. With these data we will be able to assess the quality and vulnerability of aquifers in our country. The first step in reaching this goal was to achieve adequate data for tritium, gamma emitters, basic chemistry, microelements and concentration of stable isotopes described by δ^{15}N, δ^{13}C, δ^{18}O of all major aquifers across Slovenia as this was not done systematically until now. The sampling is still going on and is expected to end in the spring of 2011. In this contribution we will present the results of tritium and gamma-ray emitters from the year 2009 and the correlations between them.

SAMPLING

Sampling locations were determined according to geological properties of Slovenia region (primary network of monitoring sites) and some sampling sites were added locally (local network of monitoring sites) in connection with other projects. The primary network covers all existing lithologies in Slovenia region to assure data quality. First sampling started in autumn of 2008. In 2009 new locations were set and their sampling was done in spring and in autumn. The sampling of 2010 is not finished yet as the autumn sampling has not yet begun. All samples are collected at least 3 days after rainfalls to prevent their possible impact on groundwater properties.

Samples are collected for tritium and gamma emitter measurements separately into 1-L polyethylene and 50-L containers, respectively. Samples for gamma emitters are acidified with nitric acid on the sampling site to a pH less than 2 in order to retain the radionuclides in the solution (ISO 2007). At the same time also the samples for determination of other parameters are taken.

METHODS

For tritium measurements, sample preparation was performed by electrolytic enrichment method, which consists of primary distillation, electrolytic enrichment and secondary distillation. Before any processing of samples in the laboratory, pH and conductivity were measured. In primary distillation 500 mL of sample is distilled in order to remove any impurities and other radionuclides that could interfere with tritium measurements. After the first distillation 1.5 g of sodium peroxide (Na_2O_2) is dissolved in 500 mL of sample aliquot to increase the conductivity to a value needed for the electrolytic enrichment process. During the electrolysis the samples are subject to a total charge of 1400 Ah and at the end their volume is reduced to approximately 15-20 mL. Samples are neutralized by adding 6 g of lead chloride ($PbCl_2$) and distilled for the second time. Each electrolytic run includes beside 15 samples also 3 spike waters for the enrichment factor determination and 2 dead water samples for background measurement. At the end an aliquot (8 mL) of the final distillate is mixed with 12 mL of scintillation cocktail (Ultima Gold or Hi Safe 3) in a 20-mL polyethylene vial and measured in the Quantulus 1220 spectrometer. Samples are measured for 300 min, spiked samples for 100 min and background waters for 1000 min. In addition to electrolysed samples also non-enriched samples are measured to assure better control of the sample preparation process and to check the measurement. The sequence of all measurements was performed three times. The minimum detectable activitiy for tritium is 52 Bq/m^3.

For measurements of gamma-ray emitters app. 50 L of sample is evaporated at a temperature of approximately 65ºC in order to obtain the dry residue which is then measured on a gamma-ray spectrometer. The spectrometer has a planar germanium detector with a crystal having a diameter of 8 cm and thickness of 3 cm. The detector has a resolution of 0.6 keV at low energies and 2 keV at 1.3 MeV and is equiped with a beryllium window. The spectrometer has a lead shielding with inner layers of 1 cm of mercury, 2 mm of cadmium and 1mm of copper. It has a cosmic veto shielding reducing the continuous background to 0.7 cps in the energy range from 5 keV to 2.8 MeV. By gamma-ray spectrometry activity concentrations of U-238, Th-234, Ra-226, Pb-210, Ra-228 and Th-228 are determined. The minimum detectable activities (decision thresholds) for these isotopes are 0.05 Bq/m^3 for Th-228, 0.25 Bq/m^3 for Ra-226, 0.3 Bq/m^3 for Pb-210, 0.4 Bq/m^3 for Ra-228, 1.5 Bq/m^3 for U-238, 4 Bq/m^3 for Th-234.

RESULTS AND DISCUSSION

Collected samples

Until now we collected 158 samples of groundwater and 2 samples of surface water (same sampling location) from 69 different locations during the years 2008 (13 samples), 2009 (104 samples) and 2010 (43 samples). Samples are obtained from springs, boreholes and wells (Table 1). Locations were sampled two times (spring and autumn), except for the 2008 where sampling begun in autumn. Starting from year 2010 new sampling sites were selected.

Tritium

In Figure 1 the results from 45 locations from 2009 are presented as they were all sampled twice, in spring (from April to July) and in autumn (from October to December). According to the average tritium activity for spring (676 ± 80 Bq/m^3) and autumn (667 ± 75 Bq/m^3) there is no significant difference between the two sampling periods. The minimal measured activity for spring period was 144 ± 29 Bq/m^3 (VR6275B) and for autumn period was 117 ± 14 Bq/m^3 (VR2253). Two locations from autumn sampling showed results below minimal detectable activity (VR6275B and VR5290A). The maximal activity was measured in one place (VP2241) for both spring and autumn period and was 1189 ± 121 Bq/m^3 and 1400 ± 131 Bq/m^3 respectively.

17 sampling sites showed statistically different tritium activities (Figure 1) between spring and autumn, among these 9 showed increased activity in spring and 8 in autumn (for 10 samples data for autumn is not available). Comparing averages values for tritium activities in different types of aquifers (fractured aquifers have an average of 680 ± 84 Bq/m^3; intergarnular aquifers 727 ± 84 Bq/m^3 and karstic aquifers 640 ± 71 Bq/m^3) we also observed no significant differences. If tritium activities are plotted on a chart (Figure 2) we can observe that in the fractured aquifers the tritium concentration has the smallest variability, while in the intergranular aquifers the variability is the largest.

From Figure 3 it follows that seasonal differences (calculated with U-test, describing the statistical significance of the difference of the measurement results) in comparison with aquifer porosity are more likely to occur on karstic and less on fractured aquifer.

Besides comparing tritium activity we also compared pH values between the two seasons and based on the statistical results from Table 2 we concluded that there are no major statistical differences. Average pH for spring and autumn are 7.6 and 7.3 respectively which is within the range of pH for groundwater which is usually between 6.0 and 8.5 (Hem 1970). In spring samples higher pH values were measured as in autumn samples.

Gamma emitters

Generally the activities of gamma emitters in the collected samples are near detection limits, so the counting statistics is the main source of uncertainty of the measurement result. To improve the counting statistics of radionuclides and to assess the activity concentration of Th-234 at the sampling time the samples were measured twice. The first measurement was performed as soon as possible after the evaporation and the second after a few half lives of Th-234. From the activity concentrations of U-235 and Th-234 at both measurement times the concentration of U-238 and Th-234 at sampling time was determined (Korun and Kovačič, submitted for publication). Because of the need of two measurements we present here only 30 results (Table 3). For these samples we present measurement results also for Ra-228, Th-228 and Ra-226 as the weighted mean of both measurements. The concentration of Th-234 was under the decision threshold in all samples. For Pb-210 and K-40 we present 94 results as their evaluation does not need two measurements. The averages of the raw observation (activities calculated from the peak areas) were converted into the expected activity values using Bayesian statistics (Korun and Maver Modec 2010) taking into account the fact that activity concentrations can not be negative. Usually the concentration of thorium in water is low, because of its low solubility, but it can increase due to formation of soluble complexes with carbonate, humic materials or other ligands in the water (Jia et al. 2008).

Correlations between radionuclides were made according to different types of aquifer porosities (fractured, intergranular and karstic). Below we present two of the most interesting results. Please note that the error bars for karstic aquifers were omitted, because of the clarity. In Figure 4 it can be observed that the correlation between Th-228 versus Ra-228 is high in intergranular and fractured aquifers, no correlation between these two radionuclides seems to occur in the karstic aquifers. The same is observed in the Figure 5 where the correlation between Ra-226 versus Ra-228 is presented.

Table 4 presents the correlation factors between radionuclides (U-238, Th-228, Ra-228 and Ra-226) for different types of aquifer porosities. For the intergranular porosity the correlations are very strong between Th-228, Ra-228 and Ra-226. A smaller correlation among these radionuclides is seen also in fractured type (this could be also because fewer samples are available for intergranular type and thus the correlation is better). The correlations among these radionuclides could be the consequence of lower permeability factor of intergranular and fractured aquifers in comparison with karstic ones, which allows the establishment of the balance between the host rock and the groundwater.

The high correlation between Th-228 and Ra-228 in the case of fractured and intergranular aquifers reflects the fact that Ra-228 is the parent radionuclide of Th-228 with a half-life of app 5.8 years. In the case of karstic aquifers the absence of correlation between these two radionuclides can be explained by the higher permeability factor and therefore the equilibrium between water and rock cannot be established.

Pb-210 and K-40 with tritium

The correlations between K-40 and Pb-210 with tritium for different types of aquifer porosities are presented on Figures 6 and 7. It can be observed that no correlation exist between before mentioned radionuclides. Intergranular types of aquifers tend to have higher K-40, whereas karstic aquifers tend to have lower Pb-210 concentration. Figures 8, 9 and 10 present the correlation between Pb-210 and K-40 for different groundwater sources. It can be seen that lower activity values of K-40 are found in springs and a slight correlation between the two radionuclides is also observed.

CONCLUSIONS

It was observed that correlations between radionuclides depend on the type of the aquifer (intergranular, fractured or karstic) as the consequence of different permeability coefficients. When the permeability coefficient is low the available time for reaching the equilibria between radionuclides in the water and rocks is longer than in the case when the coefficient is high. The strongest correlation is observed among Th-228, Ra-228 and Ra-226 in intergranular and fractured aquifers. In the case of tritium bigger variability of its concentrations in intergranular aquifer is observed while in fractured the variability is the smallest. Intergranular types of aquifers tend to have higher K-40, whereas karstic aquifers tend to have lower Pb-210 concentration. To confirm these conclusions more samples will be analysed.

REFERENCES

OJ RS 2005. Pravilnik o določitvi vodnih teles podzemnih voda.– *Official Journal of the Republic of Slovenia*. 6532.

Jia G, Torri G, Ocone R, Di Lullo A, De Angelis A, Boschetto R. 2008. Determination of thorium isotopes in mineral and environmental water and soil samples by α-spectrometry and the fate of thorium in water. *Applied Radiation and Isotopes* 66:1478-1487.

Hem JD. 1970. Study and Interpretation of the Chemical Characteristics of Natural Water. Second edition. Untited states government printing office, Washington.

ISO. 2007. Water quality – Determination of the activity concentration of radionuclides – Method by high resolution gamma-ray spectrometry. 10703:2007 (E)

Korun M, Kovačič K. (submitted for publication in *Applied Radiation and Isotopes*)

Korun M, Maver Modec P. 2010. Interpretation of the measurement results near the detection limit in gamma-ray spectrometry using Bayesian statistics. *Accreditation Quality Assurance* 15:515-520.

TABLES

Table 1

Year	Season	All samples	Springs	Boreholes	Wells	Surface water
2008	Autumn	13	1	6	6	/
2009	Spring	58	34	17	6	1
	Autumn	46	33	5	7	1
2010	Spring	43	31	9	3	/

Table 2

	Spring 2009		Autumn 2009	
	pH	Cond. (μS/cm^2)	pH	Cond. (μS/cm^2)
Average	7.6	428.9	7.3	413.5
Min	6.6	69.8	6.0	82.4
Max	9.2	1364.0	9.1	1318.0

Table 3

	U-238** (Bq/m^3)	Ra-226 (Bq/m^3)	Pb-210* (Bq/m^3)	Ra-228 (Bq/m^3)	Th-228 (Bq/m^3)	K-40* (Bq/m^3)
Average	6.00 ± 0.64	1.78 ± 0.20	5.2 ± 0.7	0.90 ± 0.2	0.20 ± 0.07	23.8 ± 2.9
Min	1.25 ± 0.50	0.20 ± 0.12	0.50± 0.25	0.11 ± 0.07	0.05 ± 0.04	1.6 ± 0.7
Max	16.9 ± 1.7	16.2 ± 0.9	32.8 ± 2.0	5.1 ± 0.3	0.95 ± 0.08	308 ± 32

*For Pb-210 and K-40 results from 94 results

**For U-238 only 20 results were available

Table 4

	Ra228-Ra226	Th228-Ra226	Th228-Ra228	U238-Ra226	U238-Th228	U238-Ra228
Fractured (10)	**0.88**	**0.88**	**0.93**	-0.35	-0.10	-0.23
Intergranular (6)	**0.94**	**0.83**	**0.97**	0.18	0.28	0.40
Karstic (14)	0.53	0.00	-0.29	0.76	0.65	0.35

TABLE CAPTIONS

Table 1 Number of all samples collected from 2008 until today according to their source.

Table 2 Average, minimal and maximal values for pH and conductivity for spring and autumn 2009.

Table 3 Average, minimal and maximal activity of gamma emitters based on 30 results.

Table 4 Correlation factors between radionuclides for different types of aquifer porosities (in parenthesis the number of samples is given).

FIGURES

Figure 1

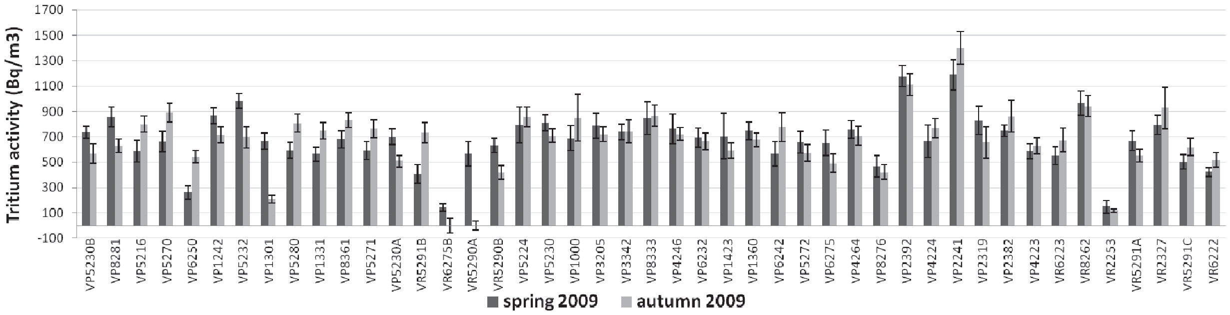

Figure 2

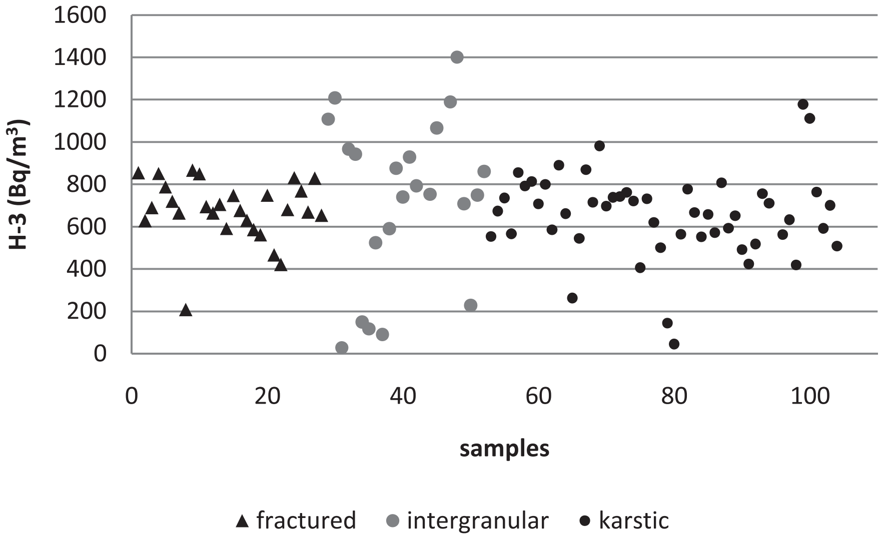
1600
1400
1200
1000
800
600
400
200
0
H-3 (Bq/m³)
0
20
40
60
80
100
samples
▲ fractured
● intergranular
● karstic

Figure 3

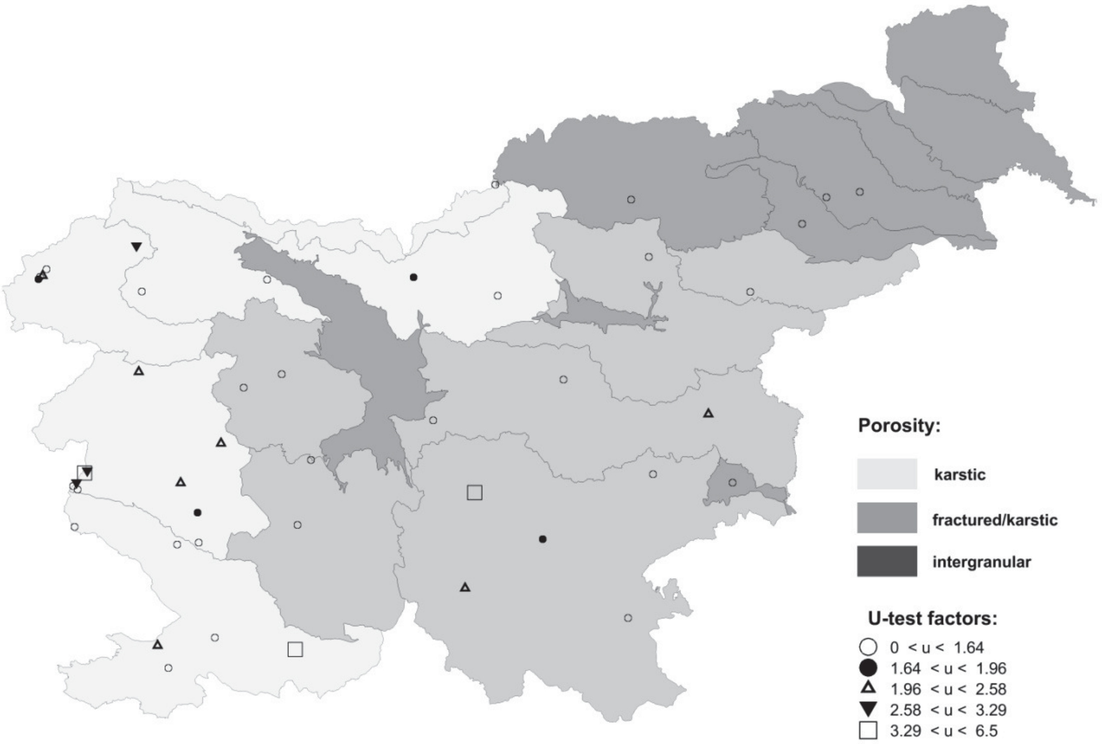
Porosity:
karstic
fractured/karstic
intergranular
U-test factors:
○ 0 < u < 1.64
● 1.64 < u < 1.96
△ 1.96 < u < 2.58
▼ 2.58 < u < 3.29
□ 3.29 < u < 6.5

Figure 4

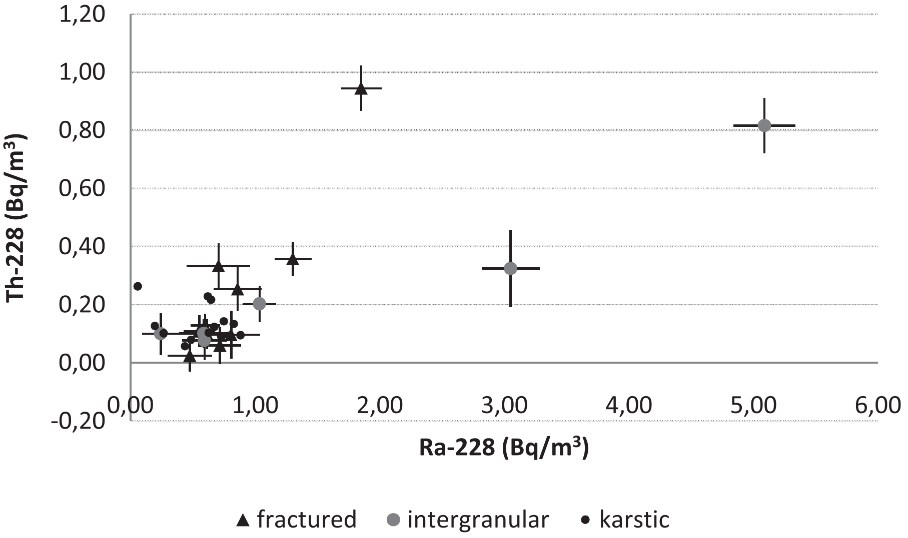
1,20
1,00
0,80
0,60
0,40
0,20
0,00
-0,20
Th-228 (Bq/m³)
0,00
1,00
2,00
3,00
4,00
5,00
6,00
Ra-228 (Bq/m³)
▲ fractured
● intergranular
• karstic

Figure 5

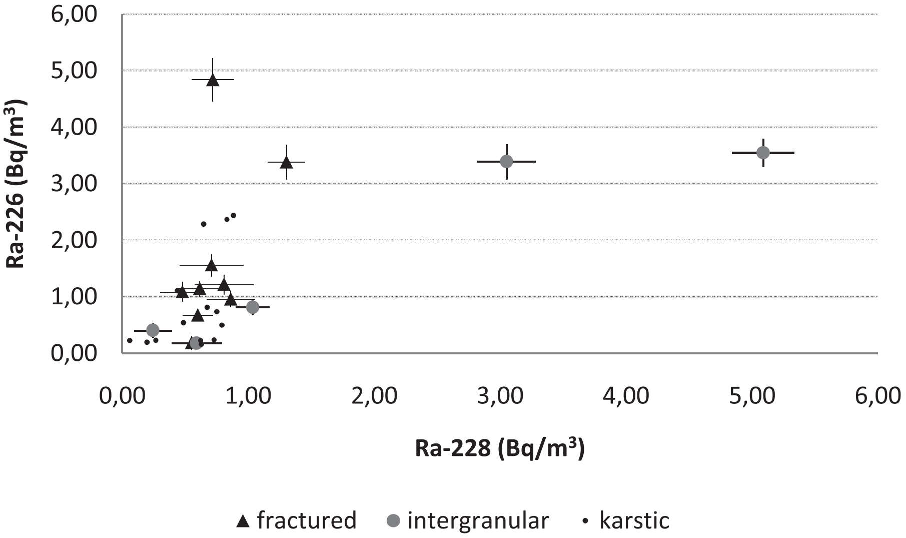
Ra-226 (Bq/m^3)
6,00
5,00
4,00
3,00
2,00
1,00
0,00
0,00
1,00
2,00
3,00
4,00
5,00
6,00
Ra-228 (Bq/m^3)
▲ fractured
● intergranular
• karstic

Figure 6

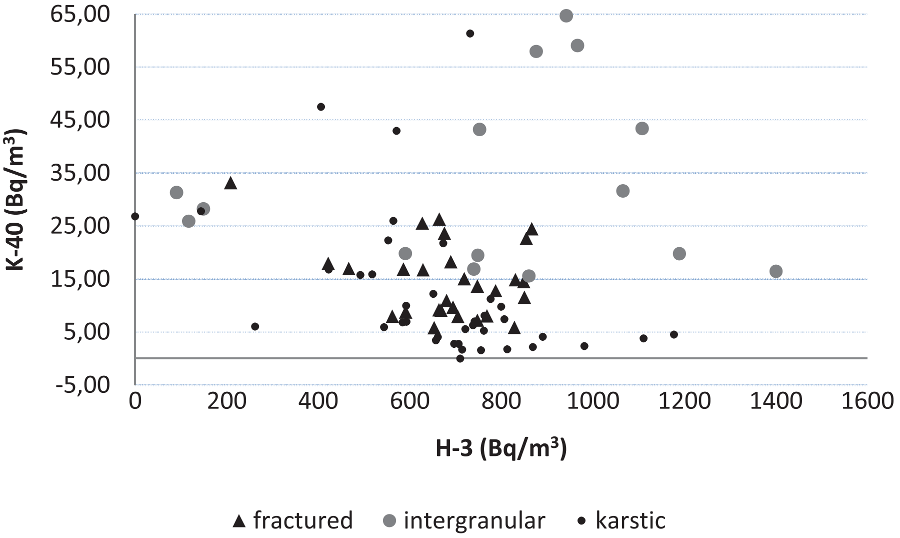
65,00
55,00
45,00
35,00
25,00
15,00
5,00
-5,00
K-40 (Bq/m³)
0
200
400
600
800
1000
1200
1400
1600
H-3 (Bq/m³)
▲ fractured
● intergranular
• karstic

Figure 7

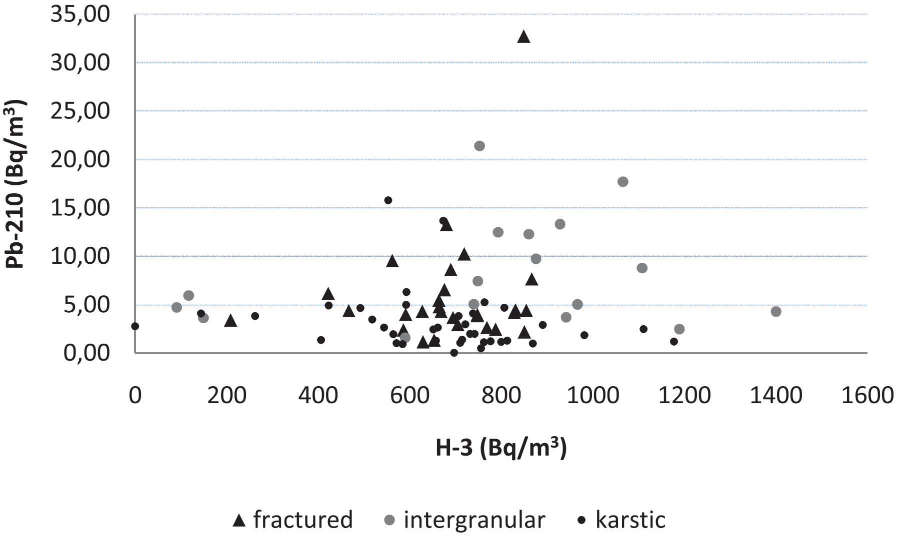
35,00
30,00
25,00
20,00
15,00
10,00
5,00
0,00
Pb-210 (Bq/m³)
0
200
400
600
800
1000
1200
1400
1600
H-3 (Bq/m³)
▲ fractured
● intergranular
• karstic

Figure 8

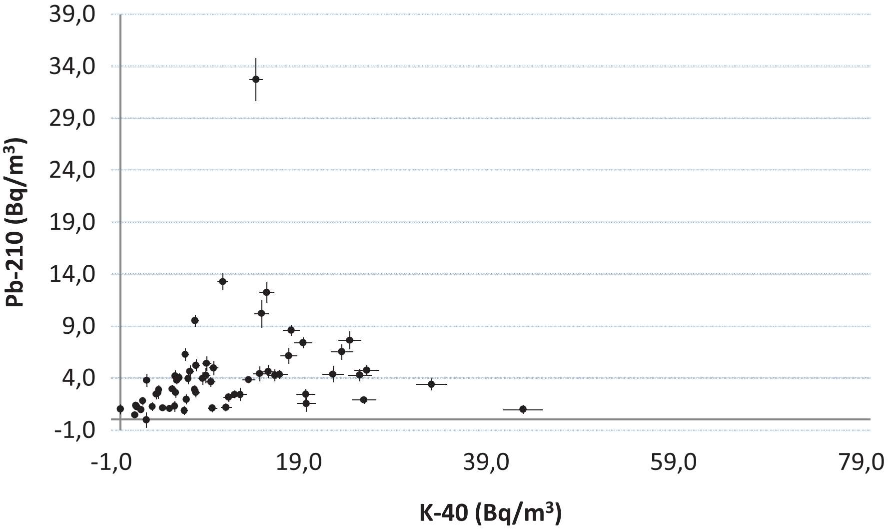
39,0
34,0
29,0
24,0
19,0
14,0
9,0
4,0
-1,0
Pb-210 (Bq/m³)
-1,0
19,0
39,0
59,0
79,0
K-40 (Bq/m³)

Figure 9

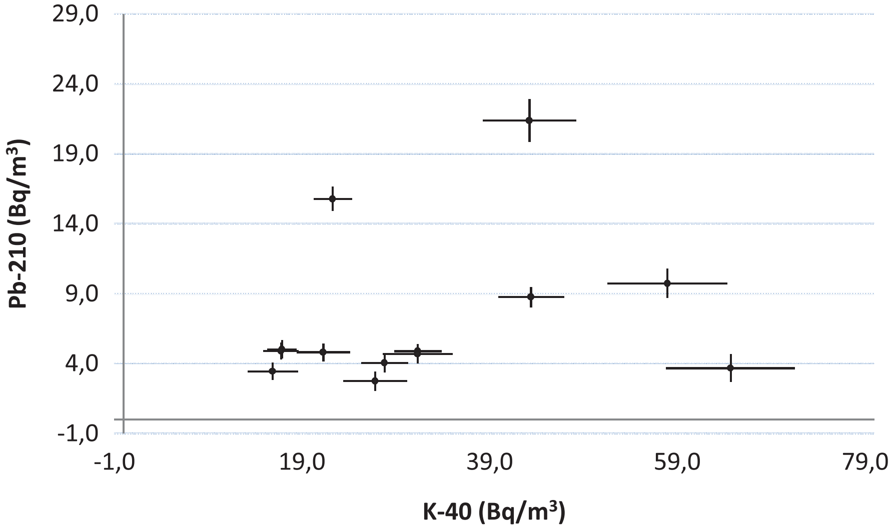

Figure 10

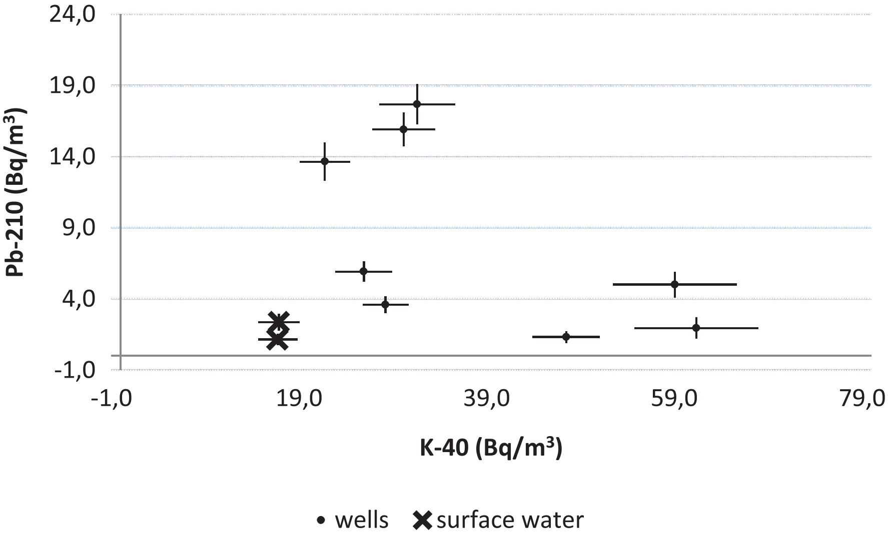

FIGURE CAPTIONS

Figure1 Tritium concentrations in groundwaters (boreholes, wells and springs) for spring and autumn 2009

Figure 2 Tritium activities (Bq/m^3) for different types of aquifer porosities

Figure 3 Seasonal differences (calculated with U-test) in comparison with aquifer porosity

Figure 4 Correlation between Th-228 and Ra-228 in different types of aquifer porosity (because of clarity error bars were omitted for samples from karstic aquifers)

Figure 5 Correlation between Ra-226 and Ra-228 in different types of aquifer porosity (because of clarity error bars were omitted for samples from karstic aquifers)

Figure 6 K-40 in correlation with H-3 for different types of aquifer porosity (because of clarity the error bars are omitted)

Figure 7 Pb-210 in correlation with H-3 for different types of aquifer porosity (because of clarity the error bars are omitted)

Figure 8 Correlation between Pb-210 and K-40 in samples from springs

Figure 9 Correlation between Pb-210 and K-40 in samples from boreholes

Figure 10 Correlation between Pb-210 and K-40 in samples from wells and surface waters

Concentration of tritium and members of the uranium and thorium decay chains in ground waters in Slovenia and their implication for managing ground-water resources

M. Korun, K. Kovačič, J. Kožar Logar

"Jožef Stefan" Institute, Ljubljana, Slovenia

Abstract. Samples of ground water were measured in terms of their activity concentration of gamma-ray emitters, members of the uranium and thorium decay chains and tritium. The distributions of the number of samples over the measured activity concentrations are presented for ^{238}U, ^{226}Ra, ^{210}Pb, ^{228}Ra, ^{228}Th, ^{40}K and ^{3}H. The distributions have three distinct shapes: lognormal distributions (^{238}U, ^{226}Ra, ^{228}Ra, ^{228}Th), bimodal distributions (^{210}Pb, ^{40}K), and a normal distribution (^{3}H). It appears that the lognormal distributions reflect the dilution of the radionuclides dissolved in the water. The bimodal distributions, being the sum of a lognormal distribution and a distribution having its maximum at the activity concentration of the higher mode, indicate influences from the soil surface, e.g. washout from the atmosphere and fertilising. The normal distribution indicates mixing with rainwater under circumstances that are characterised by several independent variable parameters.

1. Introduction

Slovenia gets a large part of its drinking water from shallow alluvial, karstic and fractured aquifers, which supply more than 97% of the Slovenian population. To manage these ground-water resources properly it is advantageous to know their properties and vulnerability that result from influences on the surface.

It is the aim of this contribution to present the first measurement results of a screening campaign for a characterisation of the ground-waters for the activity concentration of natural and anthropogenic beta particle and gamma-ray emitters.

In 2009, samples were taken at 58 locations for subsequent tritium measurements. At 49 of these locations, samples for gamma-ray spectrometric measurements were also collected. The samples were collected in both the spring and in the autumn. Here we present the results of concentration measurements for tritium ^{40}K and ^{210}Pb for all the samples collected. The measurement results for other gamma-ray emitters are presented only for the samples collected in the spring.

2. Sample preparation

The samples for the gamma-ray spectrometric measurements were prepared by the evaporation of 50 L of water using forced ventilation, as described in [1]. However, in spite of filtering the air the dry residue was contaminated by thoron daughters, i.e. thoron with a half-life of 56 s, passes through the filters and decays in the evaporation cells to its daughter ^{212}Pb with a half-life of 10.6 h. To measure the concentration of ^{228}Th in the dry residue, the daughters from the atmospheric thoron must decay before starting the measurements. In order to allow the daughter to decay before measuring the sample on the gamma-ray spectrometer the dry-residue samples were aged for at least two days.

The samples for the tritium measurements were prepared using the electrolytic enrichment method, which consists of primary distillation, electrolytic enrichment and secondary distillation. Impurities and other radionuclides that could interfere with the tritium measurements were removed by primary distillation. The electrolytic enrichment was carried out on a 500-ml sample aliquot with a prior addition of sodium peroxide (Na_2O_2). During the electrolysis the samples were subject to a total charge of 1400 Ah and at the end their volume was reduced to approximately 15-20 mL. The samples were neutralized by the addition of lead chloride ($PbCl_2$) and distilled for a second time. The aliquot (8 mL) of the final distillate with a controlled pH was mixed with 12 mL of scintillation cocktail (Ultima Gold LLT, Ultima Gold uLLT or Hi Safe 3) in a 20-mL polyethylene vial. Some 60 % of the samples were also prepared for a so-called direct measurement, where the distillate after the primary distillation was mixed with a scintillation cocktail.

3. Measurements

The gamma-ray spectrometric measurements are described in [1]. They were performed on a low-activity spectrometer having an extended range detector with a beryllium window and a cosmic veto shield. The passive shielding is made up of 15 cm of lead, 10 mm of mercury, 2 mm of cadmium and 2 mm of copper. To measure the concentration of the ^{238}U reliably, the samples were measured twice: at least two days after the evaporation and at least one month later, when the equilibrium between the ^{238}U and its daughter, ^{234}Th, is nearly achieved. Therefore, the activity concentrations of ^{226}Ra, ^{210}Pb, ^{228}Ra, ^{228}Th and ^{40}K could also be calculated more reliably, as the weighted average of the measurement results obtained from both measurements.

The spectral analysis for the activity calculation of ^{238}U and ^{226}Ra is also described in [1]. The ^{238}U activity concentration was determined from the peaks at 63 and 92 keV from the decay of ^{234}Th and the peak at 186 keV from the decay of ^{235}U assuming a natural isotopic abundance. The ^{226}Ra activity was calculated from the peaks belonging to the short-lived ^{222}Rn daughters assuming a disequilibrium between the ^{226}Ra and ^{222}Rn due to its emanation from the sample. The activity concentration of ^{228}Ra was calculated from the peaks at energies of 338 keV, 911 keV and 969 keV, and the activity concentration of ^{228}Th from the peaks at 239 keV, 583 keV and 2615 keV. Coincidence-summing effects were taken into account as described in [2]. The activity concentrations of ^{210}Pb and ^{40}K were calculated from peaks at energies at 46 keV and 1461 keV, respectively.

The tritium measurements were carried out in the Quantulus 1220 liquid-scintillation spectrometer. All ground-water samples were measured for 300 min, the spiked samples for 100 min and the background waters for 1000 min. The counting procedures started one day after the sample preparation to avoid any chemoluminiscence. The sequences of all the measurements were performed at least three times. The final results were weighted averages of the activities obtained from measurements after the electrolytic enrichment and direct measurements. The minimum detectable activity for the tritium was approximately 50 Bq/m^3.

4. Results

Using gamma-ray spectrometric measurements the activity concentrations of ^{238}U, ^{226}Ra, ^{210}Pb, ^{228}Ra, ^{228}Th and ^{40}K were measured. The activity of the ^{234}Th was measured as well, but it did not exceed the decision threshold (4 Bq/m^3) in any sample. The distributions of the number of samples over the measurement results are presented in Fig-s. 1- 6. The results are presented for samples collected in the first half of 2009, except for the results relating to ^{210}Pb and ^{40}K, where the results for all the samples collected in 2009 are presented. The bins in the figures correspond roughly to the uncertainties of the measurement results near the detection limit. In Table 1 these uncertainties are given together with the number of measurement results not present in the interval of the activity concentrations presented in the figures.

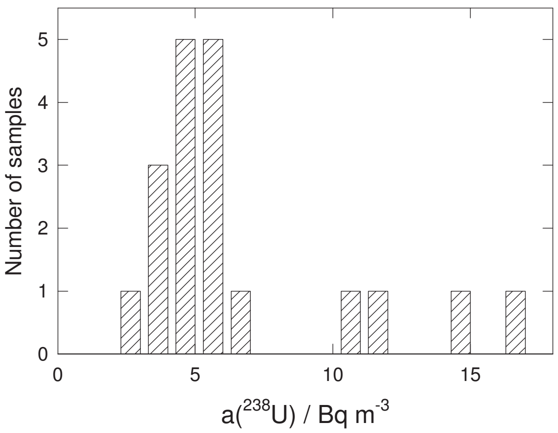

FIG. 1. The probability distribution of the number of results over the ^{238}U activity concentration.

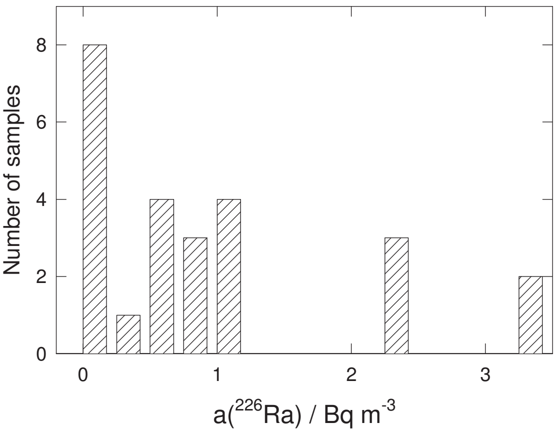

FIG. 2. The probability distribution of the number of results over the ^{226}Ra activity concentration

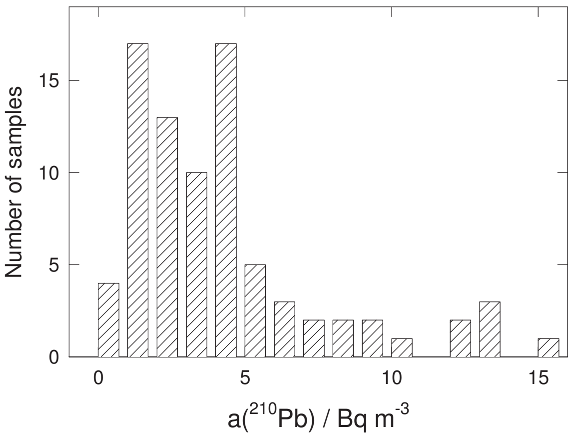

FIG. 3. The probability distribution of the number of results over the ^{210}Pb activity concentration.

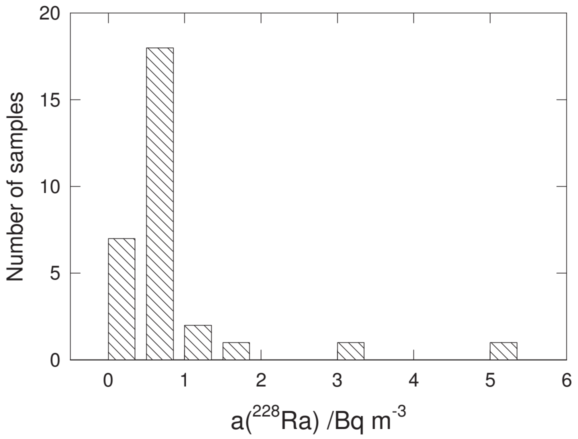

FIG. 4. The probability distribution of the number of results over the ^{228}Ra activity concentration

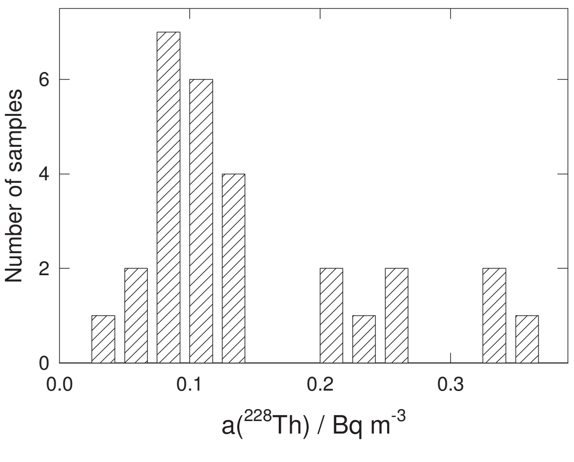

FIG. 5. The probability distribution of the number of results over the ^{228}Th activity

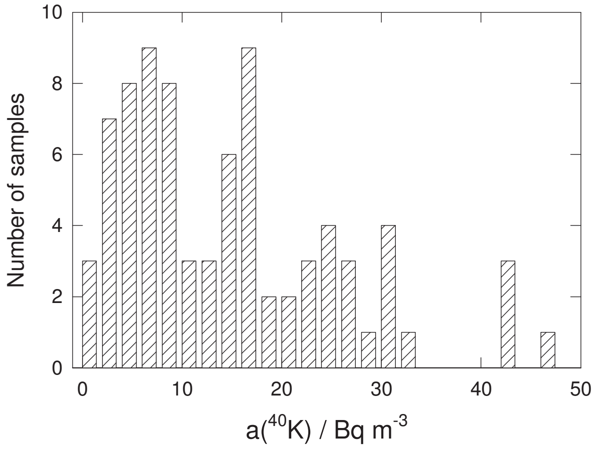

FIG. 6. The probability distribution of the number of results over the ^{40}K activity concentration

concentration.

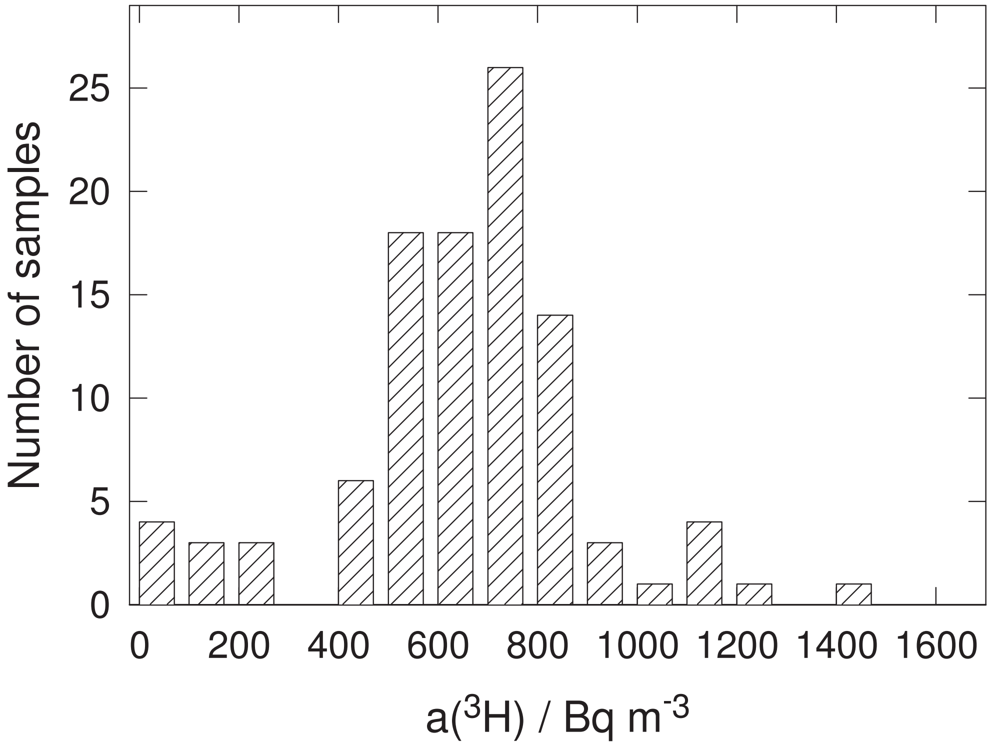

FIG. 7. The probability distribution of the number of results over the ^{3}H activity concentration

The distribution of the number of samples over the tritium activity concentration is presented in Fig. 7. Here the bin width corresponds, approximately, to the average uncertainty concentration of the activity.

Table 1. The uncertainties near the detection limit and the number of measurement results, not presented in Fig-s 1 – 6, and their average.

Nuclide	Uncertainty at MDA Bq/m^3	Number of measurement results not presented	Average activity Bq/m^3
U-238	1	0	-
Ra-226	0.15	2	11
Pb-210	0.5	3	24
Ra-228	0.15	0	-
Th-228	0.05	2	0.9
K-40	1	6	140

5. Discussion

It is clear from Fig-s 1 – 6 that the shapes of the presented distributions fall into three categories: distributions that resemble the shape of the lognormal distribution (^{238}U, ^{228}Ra, ^{228}Th); the distribution for ^{226}Ra, which falls with the activity concentration; and the bimodal distributions (^{210}Pb and ^{40}K). The host material of the Slovenian aquifers are predominantly limestone and dolomite, having a low and fairly uniform activity concentration of the members of the uranium and thorium decay chains. Frequent and large variations in the activity concentrations with respect to the sampling site are therefore not expected. Consequently, the expected shape of the distribution is lognormal, with an average activity concentration given by the solubility of the radionucleus in the water. Thus, more complicated distributions for ^{210}Pb and ^{40}K are, most probably, the result of influences of non-geological factors, caused by e.g. the intrusion of rainwater and the use of fertilizers containing potassium, respectively. For these two radionuclides the distribution is a sum of the lognormal distribution and another distribution having its maximum at the mode with the higher activity concentration. The distribution of ^{226}Ra, which does not fall off at low-activity concentrations, may reflect difficulties in the spectrum analysis originating from the time-dependent background induced by the radon-daughters [1,3].

Among the samples collected, only two exhibit enhanced concentrations of radionuclides. The measurement results for these samples are given in Table 2. It is clear that in the sample VP1000 only the activity concentration of the ^{238}U is not elevated and, in the sample VR2253, the activity concentration of the ^{210}Pb. The catchment of the sample VP1000 consists of Permo-Carbonian rocks, mainly sandstones. The tritium measurement shows that the water is recent. On the other hand, the sample VR2253 contains older water, with the tritium activity of about 150 Bq/m^3. The aquifer is made of Pliocene unconsolidated sediments, mostly sands and clays.

Table 2. Measurement results (in Bq/m^3) of two samples, exhibiting enhanced concentrations of members of the uranium and thorium decay chains

Radionuclide	VP1000	VR2253
^{238}U	2.6 ± 0.3	16.9 ± 1.7
^{226}Ra	16.2 ± 1.0	3.6 ± 0.3
^{210}Pb	8.6 ± 0.5	3.6 ± 0.6
^{228}Ra	1.9 ±0.2	5.1 ± 0.3
^{228}Th	0.95 ± 0.08	0.82 ± 0.09
^{40}K	18.2 ± 1.5	28.2 ± 2.5
^{3}H	690 ± 100	150 ± 50

Where the vulnerability of ground-water resources to influences of anthropogenic pollution is the largest can be inferred from the distribution of the activity concentrations of ^{210}Pb and ^{40}K. In aquifers where the activity concentrations of ^{210}Pb and ^{40}K are close to the maxima at the higher concentration in the bimodal distributions, i.e. 4 Bq/m^3 and 15 Bq/m^3, respectively, the vulnerability may be higher. However, to support this hypothesis additional evidence is needed, e.g. a correlation with the ^{7}Be concentration, the type of aquifer and the concentrations of chemical pollutants.

In the case of tritium the distribution is different compared to the distributions observed in gamma-ray emitters. The majority of the samples belong to a normal-like distribution with a mean value of approximately 700 Bq/m^3 and a standard deviation of around 200 Bq/m^3. The normal-like shape suggests that tritium activities in groundwater are influenced by a number of independent parameters; their variability is reflected in a distribution resembling the shape of a normal distribution. On the other hand, samples having activities less than 200 Bq/m^3, show a distribution, decreasing with activity concentration, which may resemble a log-normal distribution. These samples could represent groundwaters that were not subject to mixing since the era before the atomic bomb testing. In contrast, the activity concentrations falling within the range of the normal distribution may indicate that the corresponding groundwaters are recent.

6. **Conclusion**

It can be concluded that the relatively homogeneous radioactivity distribution of the Slovenian territory, being dominated by minerals of low concentrations of radioactive substances, reflects in distributions of activity concentrations of the members of the uranium and thorium decay chains in ground waters that exhibit a lognormal shape. The more complicated shapes are attributed to the influences from the surface, e.g. the washout of the atmosphere and anthropogenic influences. However, samples can be found with significantly increased activity concentrations, presumably reflecting specific circumstances in the corresponding aquifer.

The bimodal shape of the activity distribution of ^{210}Pb and ^{40}K may reflect influences from the earth surface on the aquifers and indicate circumstances where the increased vulnerability of ground-water resources to anthropogenic pollution can be expected.

The distribution of the number of samples over the tritium concentration exhibits a symmetrical shape, resembling that of a normal distribution. This shape is attributed to the inflow of rainwater into the aquifers under varying conditions. However, some samples exhibit a low concentration of tritium; these samples are attributed to aquifers with no mixing with the surface water at least since before the period when the atomic bomb tests were performed.

REFERENCES

[1] KORUN, M., KOVAČIČ, K., Determination of ^{238}U in ground-water samples by gamma-ray specrometry, Appl. Radiat. Isot. **68** (2011) 636.

[2] KORUN, M., MARTINČIČ, R., Activity calculation for voluminous samples in the presence of coincidence summing effects, Nucl. Instr. and Meth., A **355** (1995) 600.

[3] MAVER MODEC, P., KORUN, M., MARTELANC, M., VODENIK, B., A comparative study of the radon-induced background in low-level gamma-ray spectrometry, Ms. Ref. No. ARI-D-11-00035.